NASA Contractor Report 186025

Program for an Improved Hypersonic Temperature-Sensing Probe

Richard J. Reilly

Contract NAS2-13457
June 1993

National Aeronautics and
Space Administration

NASA Contractor Report 186025

Program for an Improved Hypersonic Temperature-Sensing Probe

Richard J. Reilly
Cuyuna Corporation
3909 Peak Lookout Drive
Austin, Texas 78737

Prepared for
Dryden Flight Research Facility
Edwards, California
Under Contract NAS2-13457

1993

National Aeronautics and
Space Administration

Dryden Flight Research Facility
Edwards, California 93523-0273

CONTENTS

ILLUSTRATIONS

TABLES

ABSTRACT

Under a NASA Dryden-sponsored contract in the mid 1960s, temperatures of up to 2200 °C (4000 °F) were successfully measured using a fluid oscillator. The current program, although limited in scope, explores the problem areas which must be solved if this technique is to be extended to 10,000 °R. The potential for measuring extremely high temperatures, using fluid oscillator techniques, stems from the fact that the measuring element is the fluid itself. The containing structure of the oscillator need not be brought to equilibrium temperature with the fluid for temperature measurement, provided that a suitable calibration can be arranged. This program concentrated on review of high-temperature material developments since the original program was completed. Other areas of limited study included related pressure instrumentation requirements, dissociation, rarefied gas effects, and analysis of sensor time response.

NOMENCLATURE

°C	degrees Centigrade
C^*	constant in thermal response calculation (defined in text)
C_p	specific heat of a gas at constant pressure
C_v	specific heat of a gas at constant volume
°F	degrees Fahrenheit
K	Knudsen number
K^*	constant in thermal response calculation (defined in text)
M	Mach number
°R	degrees Rankine
Re	Reynolds number
T	temperature
a	speed of sound
d	a characteristic dimension
e	base of natural logarithms
p	pressure
t	time
γ	ratio of specific heats, C_p/C_v
λ	mean free molecular path
ρ	gas density
τ	time constant
μ	gas viscosity

Subscripts

0	free-stream conditions
2	conditions behind normal shock
in	characteristic of gas entering temperature sensor
m	characteristic of gas inside temperature sensor
t	total (pressure, temperature)

INTRODUCTION

This program is, in a sense, a continuation of NASA effort begun more than 25 years ago. At that time, interests within NASA saw need for a temperature sensor to measure very high total temperatures in compressible gases. NASA Dryden sponsored a program with Honeywell Inc. which produced instrumentation, based on fluidic techniques, capable of measuring to a level of 2200 °C (4000 °F). For a more complete introduction to the current program a short history of the earlier NASA program is included as Appendix A.

The current program focused on the problems to be solved if this technology is to be taken to temperatures of approximately 5500 °C (10,000 °F). The most difficult area is that of material followed closely by the pressure transducer technology required to get pressure pulse signal out of the fluidic other concerns, regarding dissociation and continuum flows in rarefied environments, were explored by a limited analysis.

SUMMARY

The fluid temperature sensor is unique in that, for gaseous fluids, the fluid itself is the measuring element. As a result it is not necessary for any solid material to be brought to ultra high temperatures to accomplish a measurement. The oscillation frequency of a fluid oscillator is very nearly a linear function of the square root of the absolute temperature of the gas flowing through it. In the mid-1960s, NASA sponsored a development program which successfully measured air temperatures of 2200 °C (4000 °F) using this technology. The current program explored major questions relative to applying this technique to measure temperatures of 5538 °C (10,000 °F). Measurement of temperatures of this magnitude may be possible because the temperature gradient between the flowing fluid and survivable material temperatures is accomplished across the boundary layer of the gas.

The major objectives of this program as defined in the statement of work were:

* Define NASA areas of application for measuring ultra- high temperatures as a guide for developing a design specification
* Review progress in the development of materials for use at high temperatures
* Review developments in the field of high temperature, high frequency pressure transducers
* Explore effect of dissociation and rarefied gas effects on performance of the fluid temperature sensor

* Define potential sources for fabricating experimental temperature sensor.

NASA requirements for an ultra-high temperature sensor were explored during discussions with research personnel at Ames and at Dryden. The nature of research at both facilities demands that materials and technology chosen for an advanced capability temperature sensor must be capable of operation in an oxidizing environment. There was common interest in the rapid time response that is characteristic of the fluid temperature sensor. While measuring capability to 2500 °C (4500 °F) is adequate for materials research, re-entry instrumentation needs a 10,000 °R capability. Mach 10 in a standard atmosphere produces total temperatures in the 8,000–10,000 °R range. Considering other potential applications in the propulsion field, all NASA users work in an oxidizing atmosphere.

Materials for fabricating a 10,000 °R sensor are a difficult problem. Carbon/carbon is an attractive but disappointing option. While carbon increases in strength to temperatures of approximately 2200 °C (4000 °F), it begins to vaporize at about 425 °C (800 °F). Some refer to it as “frozen smoke.” The structural properties of carbon/carbon have spurred a great deal of work on protective coatings but no really successful coating has been developed for the oxidizing, thermal cycling environment required for temperature sensor applications.

Ceramic matrix composites present even more complex problems. The conventional considerations of strength, fatigue, bending modulus and creep resistance remain important. In addition, thermochemical compatibility between the ceramic matrix material and the reinforcing fibers comes into play. Because of the rigors of an oxidizing environment, most non-oxide materials require oxide protection systems as with carbon, especially after microcracking begins in the matrix material. As a practical matter, because of oxidation problems, potentially useful ceramics for temperature sensor fabrication are mainly limited to oxide/oxide (oxide reinforcing fibers in an oxide matrix) composites.

Pressure transducers with high frequency capability have made limited progress since the earlier NASA programs. Threshold levels and resolution have been improved. However, high temperature capability, as required for temperature sensor applications, has receded somewhat. This has occurred because, by placing emphasis on ease of use, some manufacturers are incorporating amplifier circuitry into the transducer body. This limits the operating temperature to the capability imposed by the semiconductor materials rather than the limit of the basic piezoelectric element (quartz for example). Although basic transducers are still available, the high temperature “special use” versions used previously, are no longer available.

Dissociation effects will become important somewhere in the temperature region of 2800 °C (5000 °F) and above. A limited analytical study of the dissociative effect was made by comparing the speed of sound in a gas, with γ = constant and with γ computed from tabular values in reference 1, up to 6400 °R. At this temperature, with this data source, no dissociative effects were evident. More work, with experimentally determined real gas parameters at higher temperatures, is required to adequately define the dissociative effects.

The Cuyuna Corporation has only limited capability to fabricate and test experimental temperature sensors. Discussions with several instrumentation manufacturers have determined that one major manufacturer of airborne total temperature sensors is interested in cooperating with Cuyuna in developing an advanced version of the basic sensor design. Another large aerospace company has offered a cooperative effort on material development.

Conclusions

Since transducer technology has not advanced relative to high temperature capability, effective cooling will be required to get information out of the sensor via pressure sensing techniques.

Material developments have not advanced high temperature materials to a level which will permit the fabrication of an fluid temperature sensor whose oscillation cavity operates at 5,500 °C (10,000 °F) without cooling. It may be possible to build a simple, uncooled oscillator cavity for long term operation up to 1650 °C (3000 °F). For 5–10 hour life in a cycling environment some materials may allow use of an uncooled cavity to temperatures of approximately 1900–2200 °C (3500–4000 °F).

For measurements to 10,000 °F, designs based on refractory metals, having reasonable oxidation resistance, should be explored. High thermal conductivity combined with efficient cooling of the oscillator cavity may offer the best hope for an ultra-high temperature sensor based on fluid techniques.

Recommendations

Reproduce a sensor design developed under the earlier program but using high temperature materials developed by NASA Ames material developers. Objective: reestablish the technology base and evaluate fabrication techniques needed for advanced materials.

Design a sensor cavity from a refractory metal and incorporating extensive cooling passages. Evaluate, by analysis, the feasibility of rejecting enough heat to sustain cavity surfaces to temperatures below serious oxidation levels. Conduct experimental verification. Objective: determine the potential for heat transfer techniques to support a 10,000 °F sensor for long term use.

Explore potential materials and fabrication methods with the aerospace firm which has offered to participate in a cooperative effort. Objective: obtain better, first hand knowledge of material capability and to determine suitability of various high temperature materials for diffusion bonding.

Begin a search for an oscillation detection technique which overcomes the limitations of pressure port length and temperature capability imposed by pressure transducers.

APPLICATION AREAS

Discussions with personnel at NASA Dryden Flight Research Facility and NASA Ames Research Center isolated the following application areas:

Supersonic Flight Test and Research

Atmospheric Reentry Measurements

Propulsion System Measurements

Wind Tunnel Applications (Free Stream and Boundary Layer)

Arc Tunnel Measurements Materials Research

Each of these areas has its own operational environment and related requirements. In general, the flight research application seeks the highest possible temperature capability while other measurement capabilities are more restricted and better defined physical constraints. Research

applications can also tolerate more “care and feeding” such as auxiliary cooling and pretest calibration.

Flight applications carry the usual, well defined, needs for resistance to shock, vibration etc. with pressure and temperature ranges determined by the flight envelope of the vehicle. For manned vehicles, the temperature sensor can usually be constructed using the same materials or techniques as the vehicle itself. Since the sensor is small and has no moving parts, it can be relatively massive in external configuration giving it ruggedness, strength and thermal mass without adding significant weight to a flight system. Reentry systems could possibly be designed to survive on energy sinking techniques relying only on the thermal mass of the instrument. Measurements for longer flight applications might consider periodic measurements with an extending and retracting probe with cooling applied during the retracted phase.

Wind tunnel interests expressed a need for high temperature boundary layer profile measurements which brings consideration of miniaturization and vertical cascades of individual sensors. This leads to rarefied gas considerations, i.e., the mean free path of the gas molecules relative to the size of the instrument.

The operating environment is largely oxidizing, whether in the flight atmosphere, the wind tunnel or in the propulsion setting. This severely restricts the choice of materials and requires that otherwise promising material candidates, carbon/carbon composites for example, be protected with oxidation resistant coatings.

RAREFIED GAS EFFECTS

The expressed need for reentry instrumentation and for miniaturized sensors for boundary layer measurements led to the following limited exploration of real gas effects.

Reentry conditions and flight at very high altitudes is often conducted at high Mach number which results in extremely high gas temperatures. Typically, at Mach numbers of approximately 6 and above, so called “real gas effects” come into play. At the related elevated temperatures, molecular vibration, dissociation and ionization effects become important. A rigorous discussion of these issues is beyond the scope of this program; however, a limited analysis, dealing with mostly with low density effects, was conducted for the purpose of shaping the general problem areas. As a result, conclusions from this analysis should recall the limitations and be used with care.

Calculation of Knudsen Number

The aerodynamic and heat transfer effects encountered in a flow field change when the gas no longer acts as a continuous medium and the molecular character of the gas becomes important. In general, this occurs when the mean free path, γ, of the molecules is of the same order of magnitude as some characteristic dimension in the system. This condition is sometimes described in terms of the Knudsen number, *K*, defined as:

$$K = \frac{\lambda}{d}$$

Knudsen number can be expressed in terms of the more familiar aerodynamic parameters, Mach number and Reynolds number.

$$M = \frac{V}{a} \quad \text{and} \quad Re = \frac{Vd\rho}{\mu}$$

where:

V = gas velocity

ρ = gas density

μ = gas viscosity.

Combining these relationships with kinetic theory gives:

$$\mu = \frac{1}{2} \rho \lambda a \sqrt{8/\pi\gamma}$$

and

$$K = \frac{1.25 \sqrt{\gamma} M}{Re}$$

where γ is the ratio of the specific heats of the gas.

Dividing the flow regimes in terms of Knudsen number, free molecular flow can be defined as a Knudsen number exceeding 10 and slip flow as Knudsen numbers of the order of a "few percent."(2)

Application to Fluid Temperature Sensor

Consideration was given to flight conditions within the atmosphere and for Mach numbers from 1.0 to 20.0. The Knudsen number was computed for the fluid temperature sensor using a Reynolds number based on the size of the total head port of the sensor. A spread sheet was set up to compute the various intermediate parameters as well as the Knudsen. The standard atmosphere of reference 3 was used in these computations. Because of the wide range of temperatures involved, all the commonly used "constants" were calculated as a function of temperature. These "constants" include C_p, C_v, and γ.

Data for air at elevated temperatures from reference 1 were fitted to polynomials to give the following expressions for the specific heats of air.

$$C_p = \frac{0.24275 - 1.01314'\text{E} - 04 * T + 1.35025'\text{E} - 07 * T^2}{1 - 3.335989'\text{E} - 04 * T + 4.4793'\text{E} - 07 * T^2 - 3.105338'\text{E} - 12 * T^3}$$

$$C_v = \frac{0.1742 - 7.36565'\text{E}{-}05 * T + 1.04694'\text{E} - 07 * T^2}{1 - 3.0737'\text{E} - 04 * T + 4.457474'\text{E} - 07 * T^2 - 3.62076{-}12 * T^3}$$

$$\gamma = \frac{C_p}{C_v}$$

The total pressure as a function of Mach number is given by:

$$p_{to} = p_o \frac{1}{\left[1 + \frac{\gamma - 1}{2} M^2\right]^{\left[\frac{-\gamma}{\gamma - 1}\right]}}$$

and the total temperature by:

$$T_{to} = T_o\left[1 + \frac{\gamma - 1}{2}M^2\right]$$

If it is assumed that the temperature sensor inlet will operate behind a normal shock, the following relationships apply:

$$\frac{p_{t2}}{p_{to}} = \left[\frac{(\gamma+1)M^2}{(\gamma-1)M^2+2}\right]^{\left[\frac{\gamma}{\gamma-1}\right]}\left[\frac{\gamma+1}{2\gamma M^2-(\gamma-1)}\right]^{\left[\frac{1}{\gamma-1}\right]}$$

$$\frac{T_{t2}}{T_{to}} = \left[\frac{2\gamma M^2-(\gamma-1)}{\gamma+1}\right]\left[\frac{(\gamma-1)M^2+2}{(\gamma+1)M^2}\right]$$

$$\frac{\rho_2}{\rho_o} = \frac{(\gamma+1)M^2}{(\gamma-1)M^2+2}$$

$$M_2 = \left[\frac{(\gamma-1)M^2+2}{2\quad M^2-(\gamma-1)}\right]^{\frac{1}{2}}$$

The viscosity of air was computed as a function of temperature from the following relationship:

$$\mu * 10^{10} = 0.317\ T°'R^{1.5}\left[\frac{734.7}{(T°'R + 216)}\right]$$

Atmospheric values for pressure, temperature and density were computed from the equations of reference 3. Then, using the above expressions, Knudsen numbers were calculated for various Mach numbers and altitudes. These data and intermediate values of interest are presented in tabular form in Tables 1-A, 1-B, 1-C, and 1-D for a sensor inlet opening of 0.020".

The data from these tables are plotted in figure 1, showing Knudsen number as a function of altitude and Mach number. The figure shows that the larger values of Knudsen number occur at the lower values of Mach number and the data pack very closely for Mach numbers greater than $M = 4$ or 5. This results from the assumption that the sensor will always operate behind a normal shock. Inspecting the intermediate data in the tables indicates only minor changes in M_2 beyond $M = 5$. Further, V_2 and ρ_2 conspire to hold the Reynolds number, based on sensor port dimension (0.020"), remarkably constant.

Based on the foregoing criterion for free molecular flow we see that nowhere in the altitude range to 200,000 feet and Mach number to 20 does the Knudsen number approach 10. However, the Knudsen number criterion of “a few percent” is approached for nearly all Mach numbers at altitudes in excess of 120,000–140,000 feet.

TABLE 1-A

Mach Numbers 1.0 and 2.0

h	M	Tto	Pto	M2	T2	Cp	Cv	gamma	rho2	u	d	V2	Re	K
0.00	1.0	622	4005	1.000	519	0.239	0.171	1.40	2.3780E-03	3.74E-07	0.02	1116	11814	1.25E-04
10000	1.0	580	2754	1.000	483	0.239	0.171	1.40	1.7561E-03	3.54E-07	0.02	1077	8914	1.66E-04
20000	1.0	537	1841	1.000	447	0.239	0.170	1.40	1.2670E-03	3.32E-07	0.02	1037	6590	2.25E-04
30000	1.0	494	1189	1.000	412	0.239	0.170	1.40	8.8968E-04	3.10E-07	0.02	994	4758	3.11E-04
36089	1.0	468	894	1.000	390	0.239	0.170	1.40	7.0645E-04	2.96E-07	0.02	968	3850	3.84E-04
40000	1.0	468	741	1.000	390	0.239	0.170	1.40	5.8523E-04	2.96E-07	0.02	968	3189	4.64E-04
50000	1.0	468	459	1.000	390	0.239	0.170	1.40	3.6193E-04	2.96E-07	0.02	968	1972	7.50E-04
60000	1.0	468	283	1.000	390	0.239	0.170	1.40	2.2377E-04	2.96E-07	0.02	968	1219	1.21E-03
70000	1.0	468	175	1.000	390	0.239	0.170	1.40	1.3840E-04	2.96E-07	0.02	968	754	1.96E-03
80000	1.0	468	108	1.000	390	0.239	0.170	1.40	8.5608E-05	2.96E-07	0.02	968	466	3.17E-03
82021	1.0	468	98	1.000	390	0.239	0.170	1.40	7.7761E-05	2.96E-07	0.02	968	424	3.49E-03
90000	1.0	484	67	1.000	403	0.239	0.170	1.40	5.1531E-05	3.04E-07	0.02	984	277	5.33E-03
100000	1.0	490	43	1.000	408	0.239	0.170	1.40	3.1390E-05	3.08E-07	0.02	991	168	8.79E-03
120000	1.0	520	18	1.000	433	0.239	0.170	1.40	1.2316E-05	3.24E-07	0.02	1020	65	2.29E-02
140000	1.0	557	8	1.000	464	0.239	0.170	1.40	5.1603E-06	3.42E-07	0.02	1056	26	5.58E-02
150000	1.0	575	5	1.000	479	0.239	0.171	1.40	3.4148E-06	3.51E-07	0.02	1073	17	8.52E-02
200000	1.0	548	1	1.000	457	0.239	0.170	1.40	5.6596E-07	3.38E-07	0.02	1048	3	5.06E-01
0.00	2.0	934	16556	0.577	875	0.246	0.177	1.38	6.4064E-03	5.53E-07	0.02	829	16011	5.31E-05
10000	2.0	869	11386	0.577	815	0.244	0.176	1.39	4.7201E-03	5.26E-07	0.02	801	11996	7.09E-05
20000	2.0	805	7608	0.577	755	0.243	0.175	1.39	3.3983E-03	4.98E-07	0.02	773	8800	9.68E-05
30000	2.0	741	4917	0.577	695	0.242	0.173	1.39	2.3816E-03	4.68E-07	0.02	743	6298	1.35E-04
36089	2.0	702	3695	0.577	658	0.241	0.173	1.40	1.8891E-03	4.50E-07	0.02	724	5067	1.68E-04
40000	2.0	702	3065	0.577	658	0.241	0.173	1.40	1.5649E-03	4.50E-07	0.02	724	4197	2.03E-04
50000	2.0	702	1896	0.577	658	0.241	0.173	1.40	9.6782E-04	4.50E-07	0.02	724	2596	3.28E-04
60000	2.0	702	1172	0.577	658	0.241	0.173	1.40	5.9837E-04	4.50E-07	0.02	724	1605	5.31E-04
70000	2.0	702	725	0.577	658	0.241	0.173	1.40	3.7009E-04	4.50E-07	0.02	724	993	8.59E-04
80000	2.0	702	449	0.577	658	0.241	0.173	1.40	2.2892E-04	4.50E-07	0.02	724	614	1.39E-03
82021	2.0	702	407	0.577	658	0.241	0.173	1.40	2.0793E-04	4.50E-07	0.02	724	558	1.53E-03
90000	2.0	726	279	0.577	680	0.242	0.173	1.39	1.3788E-04	4.61E-07	0.02	735	367	2.32E-03
100000	2.0	735	177	0.577	689	0.242	0.173	1.39	8.4013E-05	4.66E-07	0.02	740	223	3.83E-03
120000	2.0	780	75	0.577	732	0.243	0.174	1.39	3.3006E-05	4.86E-07	0.02	762	86	9.89E-03
140000	2.0	835	34	0.577	783	0.244	0.175	1.39	1.3854E-05	5.11E-07	0.02	786	35	2.39E-02
150000	2.0	862	23	0.577	808	0.244	0.176	1.39	9.1763E-06	5.23E-07	0.02	798	23	3.64E-02
200000	2.0	823	3	0.577	771	0.243	0.175	1.39	1.5188E-06	5.05E-07	0.02	781	4	2.18E-01

TABLE 1-B

Mach Numbers 3.0 and 4.0

h	M	Tto	Pto	M2	T2	Cp	Cv	gamma	rho2	u	d	V2	Re	K
0.00	3.0	1452	77726	0.475	1389	0.261	0.192	1.35	9.6901E-03	7.51E-07	0.02	822	17664	3.92E-05
10000	3.0	1352	53453	0.475	1294	0.258	0.190	1.36	7.1073E-03	7.18E-07	0.02	798	13174	5.26E-05
20000	3.0	1253	35719	0.475	1198	0.255	0.187	1.37	5.0921E-03	6.83E-07	0.02	774	9613	7.22E-05
30000	3.0	1153	23082	0.475	1103	0.252	0.184	1.37	3.5502E-03	6.47E-07	0.02	748	6840	1.02E-04
36089	3.0	1092	17348	0.475	1045	0.250	0.182	1.37	2.8069E-03	6.24E-07	0.02	731	5481	1.27E-04
40000	3.0	1092	14387	0.475	1045	0.250	0.182	1.37	2.3253E-03	6.24E-07	0.02	731	4540	1.53E-04
50000	3.0	1092	8900	0.475	1045	0.250	0.182	1.37	1.4381E-03	6.24E-07	0.02	731	2808	2.48E-04
60000	3.0	1092	5503	0.475	1045	0.250	0.182	1.37	8.8910E-04	6.24E-07	0.02	731	1736	4.01E-04
70000	3.0	1092	3404	0.475	1045	0.250	0.182	1.37	5.4990E-04	6.24E-07	0.02	731	1074	6.49E-04
80000	3.0	1092	2106	0.475	1045	0.250	0.182	1.37	3.4014E-04	6.24E-07	0.02	731	664	1.05E-03
82021	3.0	1092	1912	0.475	1045	0.250	0.182	1.37	3.0896E-04	6.24E-07	0.02	731	603	1.15E-03
90000	3.0	1129	1309	0.475	1080	0.252	0.183	1.37	2.0528E-04	6.38E-07	0.02	741	397	1.75E-03
100000	3.0	1144	830	0.475	1094	0.252	0.184	1.37	1.2518E-04	6.44E-07	0.02	745	242	2.88E-03
120000	3.0	1214	351	0.475	1161	0.254	0.186	1.37	4.9360E-05	6.69E-07	0.02	764	94	7.40E-03
140000	3.0	1299	158	0.475	1243	0.256	0.188	1.36	2.0807E-05	6.99E-07	0.02	785	39	1.78E-02
150000	3.0	1341	108	0.475	1283	0.258	0.189	1.36	1.3810E-05	7.14E-07	0.02	796	26	2.70E-02
200000	3.0	1280	16	0.475	1224	0.256	0.187	1.36	2.2789E-06	6.93E-07	0.02	781	4	1.62E-01
0.00	4.0	2178	321283	0.435	2099	0.279	0.210	1.32	1.2267E-02	9.67E-07	0.02	866	18291	3.42E-05
10000	4.0	2029	220948	0.435	1955	0.276	0.207	1.33	8.9808E-03	9.27E-07	0.02	842	13601	4.61E-05
20000	4.0	1879	147644	0.435	1810	0.272	0.204	1.34	6.4179E-03	8.85E-07	0.02	819	9891	6.35E-05
30000	4.0	1729	95409	0.435	1666	0.269	0.200	1.34	4.4593E-03	8.42E-07	0.02	794	7009	8.99E-05
36089	4.0	1638	71710	0.435	1578	0.266	0.198	1.35	3.5165E-03	8.14E-07	0.02	778	5601	1.13E-04
40000	4.0	1638	59469	0.435	1578	0.266	0.198	1.35	2.9131E-03	8.14E-07	0.02	778	4640	1.36E-04
50000	4.0	1638	36787	0.435	1578	0.266	0.198	1.35	1.8016E-03	8.14E-07	0.02	778	2870	2.20E-04
60000	4.0	1638	22747	0.435	1578	0.266	0.198	1.35	1.1139E-03	8.14E-07	0.02	778	1774	3.56E-04
70000	4.0	1638	14072	0.435	1578	0.266	0.198	1.35	6.8891E-04	8.14E-07	0.02	778	1097	5.75E-04
80000	4.0	1638	8707	0.435	1578	0.266	0.198	1.35	4.2613E-04	8.14E-07	0.02	778	679	9.29E-04
82021	4.0	1638	7903	0.435	1578	0.266	0.198	1.35	3.8707E-04	8.14E-07	0.02	778	616	1.02E-03
90000	4.0	1693	5410	0.435	1631	0.268	0.199	1.34	2.5759E-04	8.31E-07	0.02	787	407	1.55E-03
100000	4.0	1716	3431	0.435	1653	0.268	0.200	1.34	1.5718E-04	8.38E-07	0.02	791	247	2.55E-03
120000	4.0	1821	1451	0.435	1755	0.271	0.202	1.34	6.2137E-05	8.69E-07	0.02	809	96	6.52E-03
140000	4.0	1948	652	0.435	1877	0.274	0.205	1.33	2.6258E-05	9.05E-07	0.02	830	40	1.56E-02
150000	4.0	2012	446	0.435	1939	0.275	0.207	1.33	1.7446E-05	9.23E-07	0.02	840	26	2.37E-02
200000	4.0	1919	67	0.435	1849	0.273	0.205	1.33	2.8745E-06	8.97E-07	0.02	825	4	1.42E-01

TABLE 1-C

Mach Numbers 5.0 and 10.0

h	M	Tto	Pto	M2	T2	Cp	Cv	gamma	rho2	u	d	V2	Re	K
0.00	5.0	3112	1119554	0.415	3008	0.293	0.224	1.30	1.4227E-02	1.19E-06	0.02	933	18560	3.20E-05
10000	5.0	2898	769922	0.415	2801	0.290	0.222	1.31	1.0427E-02	1.14E-06	0.02	907	13774	4.31E-05
20000	5.0	2684	514485	0.415	2595	0.288	0.219	1.31	7.4580E-03	1.10E-06	0.02	881	9995	5.95E-05
30000	5.0	2470	332466	0.415	2388	0.284	0.216	1.32	5.1845E-03	1.04E-06	0.02	853	7065	8.43E-05
36089	5.0	2340	249884	0.415	2262	0.282	0.214	1.32	4.0884E-03	1.01E-06	0.02	836	5636	1.06E-04
40000	5.0	2340	207229	0.415	2262	0.282	0.214	1.32	3.3869E-03	1.01E-06	0.02	836	4669	1.28E-04
50000	5.0	2340	128189	0.415	2262	0.282	0.214	1.32	2.0946E-03	1.01E-06	0.02	836	2887	2.07E-04
60000	5.0	2340	79264	0.415	2262	0.282	0.214	1.32	1.2950E-03	1.01E-06	0.02	836	1785	3.34E-04
70000	5.0	2340	49036	0.415	2262	0.282	0.214	1.32	8.0096E-04	1.01E-06	0.02	836	1104	5.40E-04
80000	5.0	2340	30340	0.415	2262	0.282	0.214	1.32	4.9544E-04	1.01E-06	0.02	836	683	8.74E-04
82021	5.0	2340	27541	0.415	2262	0.282	0.214	1.32	4.5003E-04	1.01E-06	0.02	836	620	9.62E-04
90000	5.0	2419	18853	0.415	2338	0.283	0.215	1.32	2.9950E-04	1.03E-06	0.02	847	410	1.45E-03
100000	5.0	2451	11957	0.415	2370	0.284	0.215	1.32	1.8274E-04	1.04E-06	0.02	851	249	2.39E-03
120000	5.0	2601	5058	0.415	2515	0.286	0.218	1.31	7.2225E-05	1.08E-06	0.02	870	97	6.11E-03
140000	5.0	2783	2274	0.415	2691	0.289	0.220	1.31	3.0502E-05	1.12E-06	0.02	893	40	1.46E-02
150000	5.0	2875	1555	0.415	2779	0.290	0.222	1.31	2.0258E-05	1.14E-06	0.02	904	27	2.22E-02
200000	5.0	2742	233	0.415	2651	0.288	0.220	1.31	3.3397E-06	1.11E-06	0.02	888	4	1.33E-01
0.00	10.0	10892	89801418	0.387	10575	0.325	0.256	1.27	1.8682E-02	2.35E-06	0.02	1421	18850	2.89E-05
10000	10.0	10143	61756851	0.387	9848	0.323	0.254	1.27	1.3725E-02	2.26E-06	0.02	1378	13941	3.92E-05
20000	10.0	9395	41267745	0.387	9121	0.321	0.252	1.27	9.8491E-03	2.17E-06	0.02	1334	10075	5.42E-05
30000	10.0	8646	26667666	0.387	8394	0.319	0.250	1.27	6.8768E-03	2.08E-06	0.02	1287	7089	7.71E-05
36089	10.0	8190	20043676	0.387	7951	0.318	0.249	1.27	5.4406E-03	2.02E-06	0.02	1257	5637	9.71E-05
40000	10.0	8190	16622242	0.387	7951	0.318	0.249	1.27	4.5070E-03	2.02E-06	0.02	1257	4670	1.17E-04
50000	10.0	8190	10282262	0.387	7951	0.318	0.249	1.27	2.7874E-03	2.02E-06	0.02	1257	2888	1.89E-04
60000	10.0	8190	6357940	0.387	7951	0.318	0.249	1.27	1.7233E-03	2.02E-06	0.02	1257	1785	3.06E-04
70000	10.0	8190	3933302	0.387	7951	0.318	0.249	1.27	1.0659E-03	2.02E-06	0.02	1257	1104	4.95E-04
80000	10.0	8190	2433618	0.387	7951	0.318	0.249	1.27	6.5930E-04	2.02E-06	0.02	1257	683	8.01E-04
82021	10.0	8190	2209115	0.387	7951	0.318	0.249	1.27	5.9886E-04	2.02E-06	0.02	1257	620	8.82E-04
90000	10.0	8466	1512256	0.387	8219	0.319	0.250	1.27	3.9774E-04	2.06E-06	0.02	1275	411	1.33E-03
100000	10.0	8580	959079	0.387	8330	0.319	0.250	1.27	2.4250E-04	2.07E-06	0.02	1282	250	2.19E-03
120000	10.0	9105	405723	0.387	8839	0.320	0.252	1.27	9.5529E-05	2.14E-06	0.02	1316	98	5.58E-03
140000	10.0	9742	182387	0.387	9458	0.322	0.253	1.27	4.0215E-05	2.21E-06	0.02	1355	41	1.33E-02
150000	10.0	10061	124734	0.387	9768	0.323	0.254	1.27	2.6673E-05	2.25E-06	0.02	1373	27	2.01E-02
200000	10.0	9597	18679	0.387	9317	0.322	0.253	1.27	4.4060E-06	2.20E-06	0.02	1346	4	1.21E-01

TABLE 1-D

Mach Numbers 15.0 and 20.0

h	M	Tto	Pto	M2	T2	Cp	Cv	gamma	rho2	u	d	V2	Re	K
0.00	15.0	23860	1396908867	0.382	23182	0.361	0.291	1.24	2.1304E-02	3.51E-06	0.02	1869	18889	2.82E-05
10000	15.0	22219	960660702	0.382	21588	0.356	0.286	1.24	1.5536E-02	3.39E-06	0.02	1826	13959	3.82E-05
20000	15.0	20579	641941747	0.382	19994	0.351	0.281	1.25	1.1074E-02	3.26E-06	0.02	1779	10079	5.30E-05
30000	15.0	18938	414829744	0.382	18401	0.347	0.277	1.25	7.6846E-03	3.12E-06	0.02	1727	7084	7.55E-05
36089	15.0	17939	311790059	0.382	17430	0.344	0.274	1.25	6.0592E-03	3.04E-06	0.02	1693	5628	9.51E-05
40000	15.0	17940	258567831	0.382	17431	0.344	0.274	1.25	5.0195E-03	3.04E-06	0.02	1693	4663	1.15E-04
50000	15.0	17940	159946065	0.382	17431	0.344	0.274	1.25	3.1043E-03	3.04E-06	0.02	1693	2884	1.86E-04
60000	15.0	17940	98901148	0.382	17431	0.344	0.274	1.25	1.9193E-03	3.04E-06	0.02	1693	1783	3.00E-04
70000	15.0	17940	61184608	0.382	17431	0.344	0.274	1.25	1.1870E-03	3.04E-06	0.02	1693	1103	4.85E-04
80000	15.0	17940	37856230	0.382	17431	0.344	0.274	1.25	7.3426E-04	3.04E-06	0.02	1693	682	7.84E-04
82021	15.0	17940	34363958	0.382	17431	0.344	0.274	1.25	6.6695E-04	3.04E-06	0.02	1693	619	8.64E-04
90000	15.0	18544	23523945	0.382	18017	0.346	0.276	1.25	4.4386E-04	3.09E-06	0.02	1714	410	1.30E-03
100000	15.0	18794	14918987	0.382	18260	0.346	0.277	1.25	2.7085E-04	3.11E-06	0.02	1722	250	2.14E-03
120000	15.0	19944	6311234	0.382	19378	0.350	0.280	1.25	1.0714E-04	3.21E-06	0.02	1760	98	5.45E-03
140000	15.0	21340	2837122	0.382	20734	0.353	0.283	1.25	4.5353E-05	3.32E-06	0.02	1802	41	1.30E-02
150000	15.0	22039	1940306	0.382	21413	0.355	0.285	1.24	3.0169E-05	3.37E-06	0.02	1821	27	1.96E-02
200000	15.0	21023	290557	0.382	20426	0.353	0.283	1.25	4.9626E-06	3.29E-06	0.02	1792	4	1.19E-01
0.00	20.0	42014	10120762404	0.380	40832	0.423	0.354	1.19	2.6055E-02	4.68E-06	0.02	2037	18901	2.75E-05
10000	20.0	39125	6960095207	0.380	38025	0.412	0.342	1.20	1.8548E-02	4.52E-06	0.02	2040	13963	3.74E-05
20000	20.0	36236	4650940408	0.380	35217	0.401	0.331	1.21	1.2943E-02	4.34E-06	0.02	2030	10079	5.19E-05
30000	20.0	33348	3005488314	0.380	32410	0.391	0.321	1.22	8.8145E-03	4.17E-06	0.02	2008	7081	7.41E-05
36089	20.0	31589	2258954168	0.380	30701	0.385	0.315	1.22	6.8784E-03	4.05E-06	0.02	1988	5625	9.35E-05
40000	20.0	31590	1873353121	0.380	30702	0.385	0.315	1.22	5.6981E-03	4.05E-06	0.02	1988	4660	1.13E-04
50000	20.0	31590	1158827295	0.380	30702	0.385	0.315	1.22	3.5240E-03	4.05E-06	0.02	1988	2882	1.82E-04
60000	20.0	31590	716549978	0.380	30702	0.385	0.315	1.22	2.1788E-03	4.05E-06	0.02	1988	1782	2.95E-04
70000	20.0	31590	443289393	0.380	30702	0.385	0.315	1.22	1.3475E-03	4.05E-06	0.02	1988	1102	4.77E-04
80000	20.0	31590	274272661	0.380	30702	0.385	0.315	1.22	8.3353E-04	4.05E-06	0.02	1988	682	7.72E-04
82021	20.0	31590	248970755	0.380	30702	0.385	0.315	1.22	7.5713E-04	4.05E-06	0.02	1988	619	8.49E-04
90000	20.0	32653	170433639	0.380	31735	0.389	0.318	1.22	5.0699E-04	4.12E-06	0.02	2000	410	1.28E-03
100000	20.0	33094	108089742	0.380	32163	0.390	0.320	1.22	3.1019E-04	4.15E-06	0.02	2005	250	2.10E-03
120000	20.0	35119	45725604	0.380	34131	0.397	0.327	1.21	1.2429E-04	4.28E-06	0.02	2023	98	5.35E-03
140000	20.0	37577	20555268	0.380	36520	0.406	0.336	1.21	5.3516E-05	4.42E-06	0.02	2036	41	1.27E-02
150000	20.0	38808	14057739	0.380	37717	0.411	0.341	1.20	3.5930E-05	4.50E-06	0.02	2039	27	1.92E-02
200000	20.0	37018	2105118	0.380	35977	0.404	0.334	1.21	5.8321E-06	4.39E-06	0.02	2034	4	1.16E-01

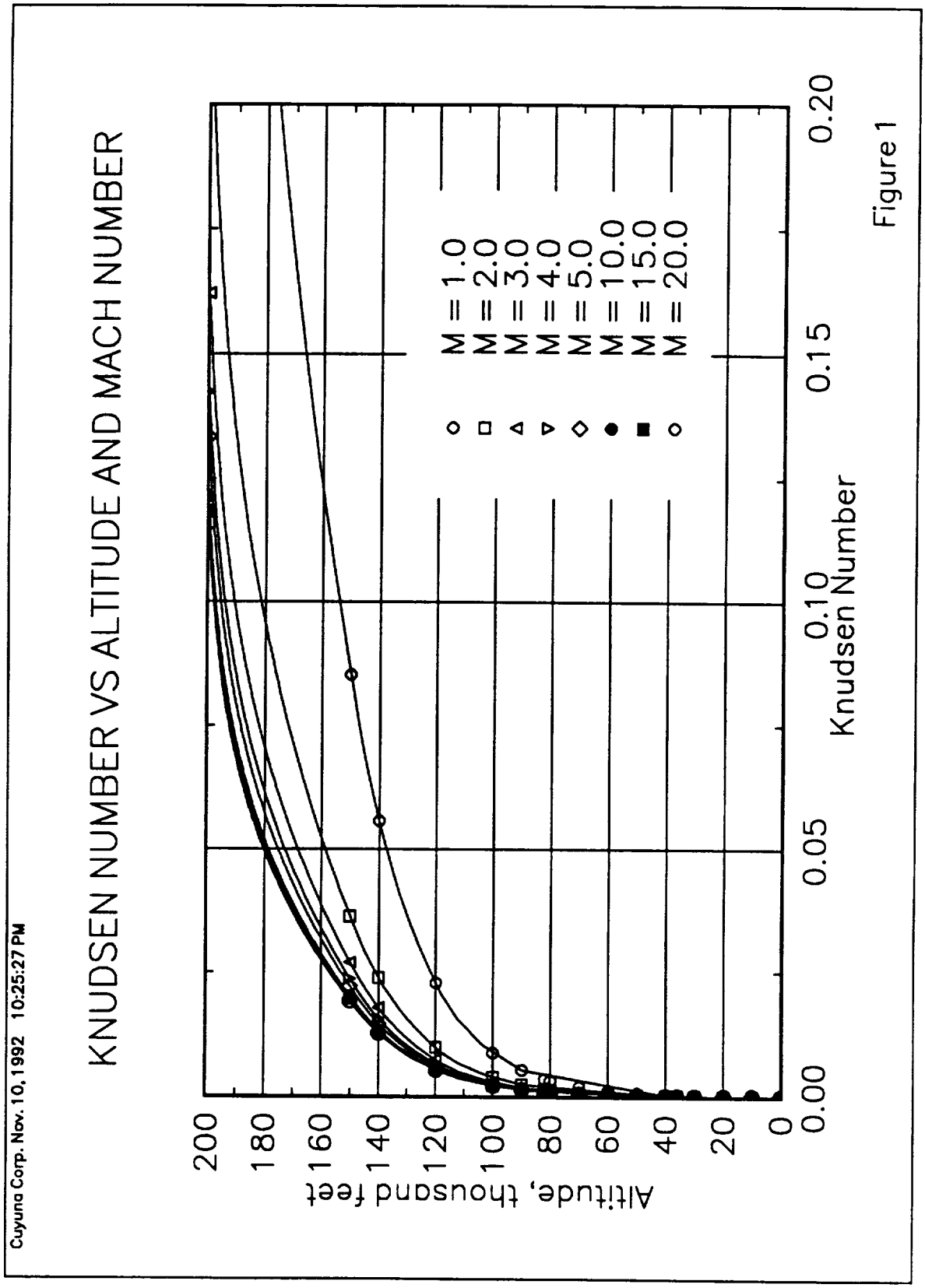
KNUDSEN NUMBER VS ALTITUDE AND MACH NUMBER
Cuyuna Corp. Nov. 10, 1992 10:25:27 PM
Altitude, thousand feet
200
180
160
140
120
100
80
60
40
20
0
0.00
0.05
0.10
0.15
0.20
Knudsen Number
M = 1.0
M = 2.0
M = 3.0
M = 4.0
M = 5.0
M = 10.0
M = 15.0
M = 20.0

Figure 1

MATERIAL EXPLORATIONS

A successful ultra-high temperature probe will depend on the proper choice of materials. U.S. Air Force interest in light weight ceramics for gas turbine engine applications dates to the 1950s.(4) In 1985, the Air Force sponsored work on ceramic composites in support of the Integrated High-Performance Turbine Engine Technology (IHPTET) initiative. This work, sponsored by Wright Laboratory, has a goal of developing materials capable of operating at 1650 - 2200 °C (3000 - 4000 °F). Two major areas of exploration have evolved: carbon/carbon composites and ceramic matrix composites.

Carbon/Carbon Composites

Carbon/carbon has received much research attention in recent years because of its extreme strength and retention of its structural properties at very high temperatures. The covalent bonds that exist between arrays of carbon atoms are among the strongest bonds known(5). These bonds are responsible for carbon's strength and stiffness. Carbon/carbon composited systems consist of high strength carbon fibers in a carbon matrix formed by carbonization of an organic binding material or by deposition of pyrolytic carbon. The resulting material is of high interest for aerospace structures because, at temperatures above 1000 °C (1830 °F), carbon/carbon's strength/density ratio exceeds that of both superalloys and ceramics. Further, in contrast to other materials, its mechanical strength improves with increasing temperature up to approximately 2200 °C (4000 °F). Other desirable characteristics include very low thermal expansion in the direction parallel to the atom layers and a relatively low vapor pressure up to temperatures of nearly 2760 °C (5000 °F).

The primary downside of carbon/carbon is the fact that it oxidizes rapidly at temperatures in excess of about 425 °C (800 °F). A wide variety of protective coating systems has been devised to facilitate the use of carbon/carbon at very high temperatures. However, controlling the variable chemical kinetics of reactions over a wide range of temperatures places sometimes conflicting requirements on the characteristics of the protective coating systems. Nevertheless, the attractive structural capability of the base material has spurred extensive research for the “holy grail” of coatings. The result has been elaborate, multi-layer coating schemes with each layer bringing its own accompanying difficulties.

The major requirements for a protective system are:

An effective oxidant barrier

An effective barrier to outward diffusion of carbon

Compatible coefficient of thermal expansion

Chemically compatible bonding over the temperature range

Oxidation of Unprotected Carbon/Carbon and Barrier Considerations

The oxidation rate of unprotected carbon/carbon composites increases rapidly (almost logarithmically) between temperatures of approximately 315 °C (600 °F) and 760 °C (1400 °F). Above 980 °C (1800 °F), the surface recession rate, while high, is almost constant with increasing temperature. Three gaseous kinetic regimes determine the rate of oxidation:

Surface reaction limitation

Limitation due to a mixture of pore diffusion and surface reaction

Limitation due to gas diffusion across the boundary layer

Between 425 °C (800 °F) and 760 °C (1400 °F) the rate of surface reaction is so rapid that the oxidants combine with the carbon substrate immediately upon crossing the boundary layer. At the higher temperatures, the rate of oxidation is limited by the ability of the gas phase diffusion to transport the oxidants. In the high temperature case, nearly all the reaction takes place at the surface of the structure and the interior is virtually unaffected. At lower temperatures, the kinetics of the oxidation reaction are much slower than the rate of diffusion of oxidants through the boundary layer. As a result, oxidants entering the porous carbon/carbon matrix can diffuse deeply into the substrate material. Thus, any protection system must create an oxidant barrier across a wide range of temperatures. Silica-based coating systems seem to have the most promise for preventing mass loss of the carbon/carbon by evaporation.

Coefficient of Thermal Expansion Considerations

Carbon/carbon is a highly unusual material from the standpoint of its thermal expansion properties. Its anisotropic structure creates a coefficient of thermal expansion (CTE) which is actually negative along the longitudinal axis of the yarn bundle and positive in the transverse direction. As a result, a coating which matches the CTE at the surface of the material will be a very poor match at the edges. The resulting internal stresses can lead to spalling of the coating material. This has special significance for the fluid temperature because cutting flow contours in the material will open material edges in areas requiring critical dimensional control. Spalling, with resulting loose particles, would likely destroy functional capability of the sensor. Some protective systems employ multiple layers of different materials with gradation of CTE which reduces the interfacial shear stresses but the tensile stresses which cause cracking remain.

Silicon carbide is the major constituent of many current protective systems because it is chemically compatible with carbon/carbon at very high temperatures and also an effective barrier to the outward diffusion of carbon. Although silica-base coatings tend to crack after application due to CTE differences, these cracks tend to close because the CTE is higher for the coating than the base material. Further, a SiO_2 glass forms at the higher temperature and helps to seal the cracks to prevent ingress of oxygen. The glass is brittle, however, and the cracks reopen again as the system is cooled. Modification of the carbon/carbon substrate to include silicon carbide tends to increase the CTE of the substrate. This makes it easier to match the characteristics to the substrate and the coatings.

The use of borate and phosphate glasses to protect carbon from oxidation has a long history.(5) Boria base glasses seal cracks and other coating imperfections at the lower temperatures before the SiO_2 glass forms. Viscosity reducers may be used to enhance the ability of the glasses to flow into the cracks. However, the rate of oxygen permeation is roughly proportional to the viscosity of the glass so the improved crack filling with viscosity reducers comes at the expense of a lowered ability to prevent oxygen diffusion into the substrate.

A further problem with the boron based glasses is that of reaction with water. Even at low temperatures, B_2O_3 films react with water forming orthoboric acid. At higher temperatures, the acid releases water vapor, forming bubbles in the coating or worse, the spalling of the surface.

Various inhibiting techniques have been explored but no totally successful solution has been isolated.

For a fluid temperature sensor, the cyclic nature of its use is also its Achilles heel. Some of the above protective systems have some capability of getting protected materials to a high temperature, and sustaining them there, on a one-time basis. However, some of the layered protection systems are dissipated in passing through the temperature range and may not be effective for the multiple excursions required of a practical sensor.

In summary, the silica-base coating systems, using SiC or Si_3N_4, appear to have the ability to protect against significant carbon mass loss to temperatures of about 1650 °C (3000 °F). Initial protection by boria glasses begins at about 425 °C (800 °F) and is effective to about 950 °C (1750 °F). Despite all the effort expended in the field, there is no completely competent protective system for carbon/carbon at ultra high temperatures.

Application of Carbon/Carbon to the Temperature Sensor

In the past, successful temperature sensors have typically involved “two-dimensional” flow passages (small depth to width ratio) cut into thin plates of the chosen material. If similar designs were to be built, fabrication of a temperature sensor from carbon/carbon requires several steps:

Formation of wafers approximately 0.020 - 0.060 of an inch thick

Cutting accurate outlines of the sensor in a wafer or cavities closed on one side in thicker material

Closing the cavity with one or two cover plates depending on the design technique chosen

Fastening the cover plates on the contoured layer by a bonding technique not yet determined.

In addition to the high temperature capability of carbon/carbon, the strength of the material is of interest for temperature sensor applications. The goal of a 10,000 °R sensor requires cooling of the sensor body and the resulting temperature gradients will induce high internal stresses in any material used. In contrast to homogeneous materials, carbon/carbon is anisotropic, displaying much greater strength in the direction of the reinforcing fibers than across fiber layers. This weakness has been addressed by material manufacturers who weave what are termed multi-dimensional materials. Unlike simple woven cloth-like reinforcing materials, these materials have contiguous fibers in many directions and approach isotropy in physical and mechanical characteristics. The figures below illustrate these multi-dimensional reinforcement techniques.

Cutting the internal contours of the fluid passages creates a special problem for these anisotropic carbon/carbon structures. Although the individual layers used in fabricating a temperature sensor can be formed from multi-dimensional blocks of carbon/carbon, the internal passages will necessarily interrupt the continuous fibers and compromise the structural integrity of the individual layers.

Joining the individual layers of a sensor is a further problem in the fabrication of a carbon/carbon temperature sensor. Most joining of load-carrying structures has used mechanical means, i.e., carbon/carbon bolts. This does not appear practical for the small parts used in temperature sensor. We have encountered some indications that there is research work in progress using eutectics of

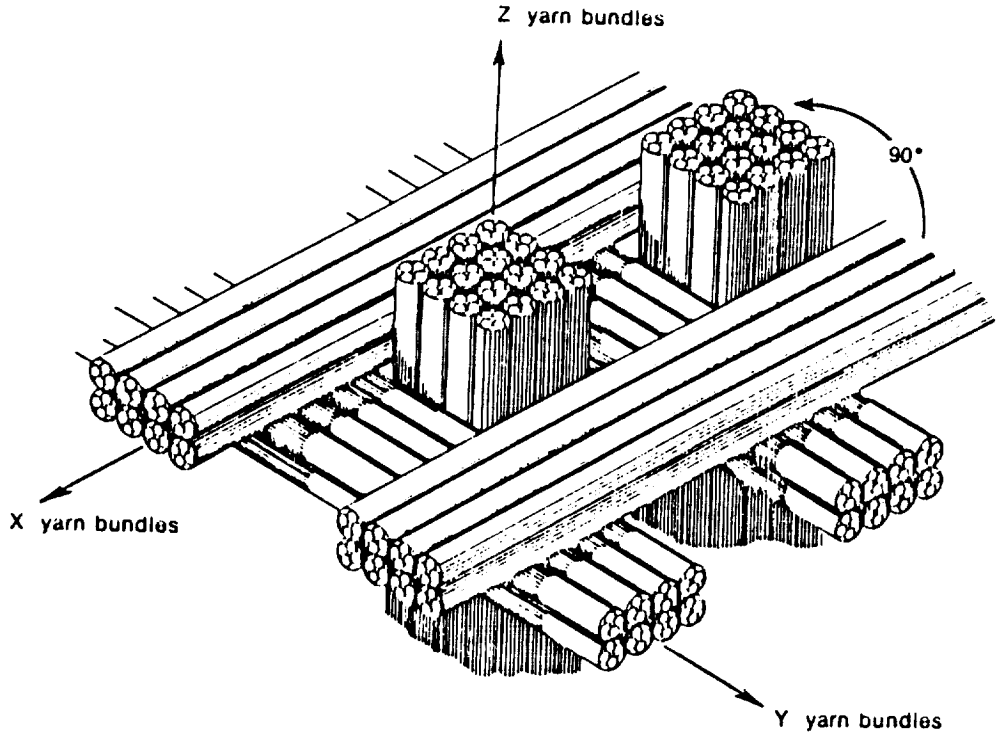

Figure 2: 3-D Orthogonal Weave

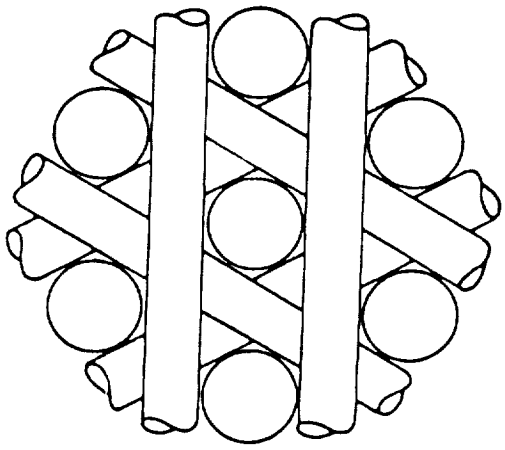

Figure 3: 4-D Hexagonal Array

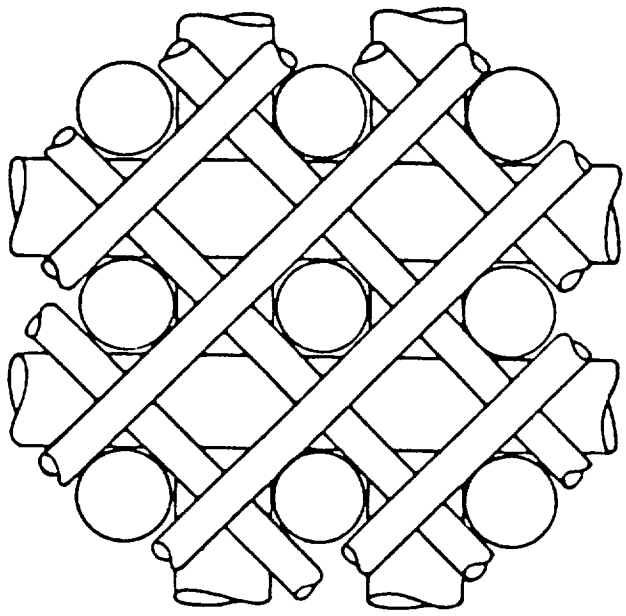

Figure 4: 5-D Weave

some sort, but the eutectics are acknowledged to be less structurally capable than the base material. No literature citations of carbon/carbon bonding were encountered.

The details of fabricating a temperature sensor from carbon/ carbon were discussed with Fiber Materials Inc. of Biddeford, Maine, a manufacturer of carbon/carbon recommended by Wright Laboratory personnel. In general, Fiber Materials was pessimistic about the use of carbon/carbon in the operational environment required by a practical temperature sensor. In particular, the cyclic nature of flight and wind tunnel testing is not compatible with carbon/carbon protection systems.

Ceramic Matrix Composites

The ability of ceramics to survive ultra-high temperatures makes them attractive to designers of gas turbines and other high temperature systems. When using a brittle material in a structural application, however, some means must be found for achieving tolerance to thermal shock, rapid fracture and potential impact damage. Ceramic matrix composite materials are fundamentally a method of alleviating the brittle fracture characteristics of ceramics. They are engineered, two-phase systems consisting of ceramic fibers, whiskers platelets or oriented particulates in a ceramic matrix.

Toughness Considerations

A temperature sensor will be exposed to cyclic high temperature operation. While a temperature sensor will not be subjected to the high centrifugal loads as encountered by some gas turbine components, the repetitive thermal strains will initiate microcracking in the ceramic matrix. This microcracking is controlled by flaws in the matrix such as pores and inclusions and by the reinforcing fibers, whiskers and platelets.

For the reinforcing fibers to accomplish this failure control function, the bond between the fiber and the matrix must meet carefully controlled conditions. First, the matrix and the reinforcing fiber must be thermochemically compatible. In addition, the fiber/matrix bond cannot be overly strong. If the bond is very strong, the material is likely to fracture catastrophically in a manner similar to the matrix material. If the interface bond is less strong, cracks do not readily propagate from one material phase into the other and the bulk material will tend to resist crack growth.

After microstructure cracking, the reinforcing fibers impart toughness to the structure through two mechanisms. Fibers by-passed by the crack planes pick up the loads shed by the matrix and fibers broken some distance from the crack planes resist opening of the crack due to frictional forces as the broken ends pull out of the matrix material. After initial cracking, the reinforcing fiber becomes vulnerable to oxidation and other environmental effects, as discussed in the section on carbon/ carbon.

A generalized stress/deflection curve is shown in Figure 5.

The load/deflection curves for a typical ceramic matrix material are characterized by an initial inelastic region and, with increasing load, a nonlinear load increase to some maximum value followed by a continuous load decrease. This noncatastrophic decrease in load gives fiber-reinforced ceramics the appearance of toughness.

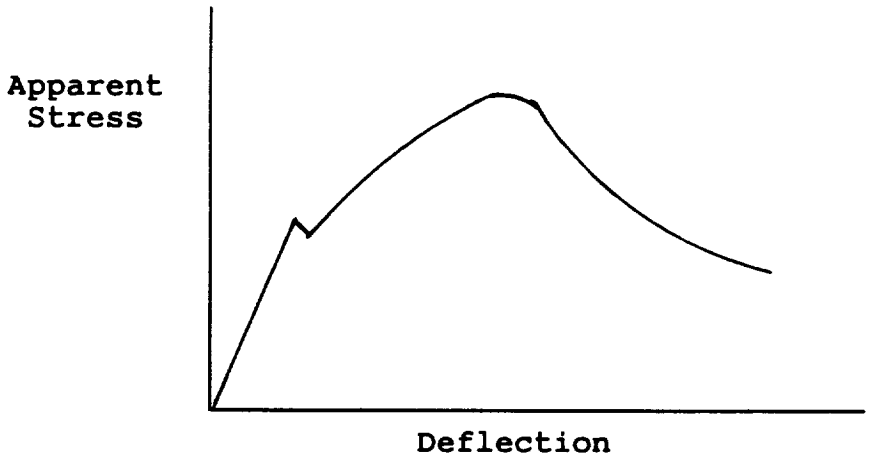

Figure 5. Load Deflection Behavior of Fiber-reinforced Ceramic Matrix Composites (From Reference 4)

Unlike structural alloys, the work of fracture (the area under the above curve) does not provide a means of predicting failure of the material independent of loading considerations. Comparisons of stress/deflection curves show large differences from sample to sample so analytical models are difficult to construct. Failure prediction from a representative sample of material is not currently possible. As a result, failure prediction for ceramics and ceramic matrix materials must often resort to statistical methods.

Creep Resistance

In general, creep resistance is not likely to be a major factor in choosing a temperature sensor material. The temperature sensor will not be subjected to rotational forces and certain other design factors will keep the unit stress levels relatively low except for thermally induced stresses. As in the discussion of toughness, creep behavior of a material is difficult to predict but fiber volume and fiber aspect ratio are thought to be of dominant importance.

As with metallic systems, creep considerations are important primarily at high temperatures. Similar to toughness calculations, computational prediction of creep involves several assumptions and the results are not totally satisfactory at this time. Typically, analytical considerations assume that the matrix and fiber are creeping at the same rate and that there is no interfacial slippage between the matrix and the reinforcing fiber. Experimentally, the performance of single crystal reinforcing fibers is significantly better than that of polycrystalline fibers. Load transfer from the matrix to the fiber is fairly constant after the fiber volume reaches 30%.

Fatigue

Time-dependent loss of strength and ultimate failure of ceramics involves entirely different mechanisms than those which occur in metals and alloys. In the latter, fatigue cracks are initiated in regions of high strain concentration which may arise from flaws in the material, from improper design or poor manufacturing execution of a design detail. In studies of crack propagation in ceramics (6) it was found that early compression cycles cause significant damage, i.e., microcracks which merge to form fatigue flaws after tens of thousands of cycles. These tests, with SiC whiskers reinforcing Si_3N_4, show the silicon carbide fibers lowered the fatigue resistance of unreinforced matrix.

Slippage between the fiber and the matrix at higher stress levels after crack initiation will probably lead to further fatigue damage. In addition, the cracking opens the way for further environmental damage to the reinforcing fiber, due to oxidation as discussed above.

Currently, the data base on fatigue limitations for ceramic composites is extremely limited. However, it appears that for reasonable fatigue resistance the design stress may have to be limited to a value below the matrix cracking stress which is significantly below the ultimate stress; perhaps as low as 2/3 the ultimate strength. Currently, design guides for ceramic materials are based primarily on strength and toughness considerations but fatigue concerns must be added to achieve a valid design analysis.

Oxidation

Ceramic matrix composites are subject to limitations due to oxidation and other environmental degradation at high temperatures. Most of the discussion presented in the section on carbon/carbon applies to ceramics. Protection of the reinforcing fiber after micro-matrix cracking is an additional complication where an environmentally sensitive reinforcing fiber is used while relying on the protective qualities of the matrix. For gas turbine applications a goal for linear recession rate has been established at less than 0. 1 μm/hr. (4) This implies a loss of 4 mils in 1000 hour which would likely be unacceptable for a temperature sensor application over that period. It would probably be acceptable, however, for 100 hours use (0.4 mils) which would be a reasonable life for a laboratory instrument.

Strength

From the standpoint of temperature sensor application, thermal transients and the resulting internal, material temperature gradients will produce the maximum stresses. As with metals and alloys, polycrystalline ceramics lose strength rapidly with increasing temperature. Since grain boundaries are an important factor in yielding of these materials, consideration should be given to using single crystals, especially for miniature sensors. Gains due to the use of single crystals will still be compromised by the need for at least one diffusion bond because of the need for internal access to create the temperature sensor flow passages.

Polycrystalline considerations are also important because of diffusion-controlled processes. Impurities can cause a glassy phase to form at grain boundaries at high temperatures. These glassy boundaries allow interfacial slippage between crystals and greatly compromise the basic material strength. This is another reason to consider the fabrication of small devices from single crystal materials.

Material Candidates

The Air Force programs studied several classes of materials for their potential use as both bulk matrix and reinforcing elements. These included:

Beryllides

Borides

Carbides

Nitrides

Oxides

Silicides

In addition to looking at the tensile strength, elastic modulus and creep resistance of these materials, consideration was given to thermochemical compatibility. For composites, the details of the bond between the reinforcing fiber and its host matrix are extremely important. As discussed earlier, toughness issues seek a relatively weak interfacial bond and minimal thermochemical activity at the bond. Optimizing the composite properties often involves coating the fibers or otherwise modifying its surface.

The Air Force studies concentrated on three general classes of reinforcement/matrix:

non-oxide/non-oxide

oxide/oxide

non-oxide/oxide.

For use in an oxidizing environment, protecting materials from oxidizing reactions has proven to be a real struggle. For example, carbon is unique among all materials in its increasing strength with increasing temperature. However, as discussed in the preceding section, the oxidation resistance of carbon is unacceptable and no satisfactory protection method has yet been developed. Without going into a detailed report of all of the materials reviewed, we quote the Air Force assessment report (4) which, after 6 years of effort, concludes: “For long term applications, only oxide/oxide composites will be able to survive in oxidizing environments.”

While this determination was based on the requirements of gas turbine engines, it is likely a valid conclusion for temperature sensor applications also. While the temperature sensor is not subject to the stresses of rotational loading, even a useful laboratory instrument will be subjected to many thermal cycles. It is this cycling that creates the most difficult problems for the oxidation protection systems that have been proposed and investigated to this time.

Long Term Material

In general, single crystal oxide fibers appear to offer the most promise although some hope for silicon carbide exists among investigators in the field. The results of many of the material tests appear to suffer from the impurities found in commercial- grade materials and a proper assessment of silicon carbide cannot be made until high temperature strength properties can be made to approach theoretical values. Silicon carbide survives at high temperatures because of the formation of a SiO_2 scale which protects the base material from oxygen permeation. Survival of this scale in

the presence of a flowing fluid is an issue to face when evaluating silicon carbide for temperature sensor fabrication. Since the sensor will likely operate behind a normal shock at high flight velocities, the worst case from the standpoint of scrubbing the protective oxide layer will probably occur at $M = 1.0$ and high gas density. Higher Mach numbers produce a stronger shock with a resulting lower velocity behind the shock.

Air Force studies highlighted BeO, Al_2O_3 and YAG (yttria aluminum garnet) in single crystal fiber configuration as capable of achieving acceptable creep rates for use in gas turbine engines. When fabricated into composites, however, some loss of single crystal properties occurs. A eutectic composed of Al_2O_3/YAG is highlighted as promising, in reference 4, with the caution that fracture toughness needs to be improved.

Conclusions regarding the flow effect on material survival must be drawn with caution. While protective oxide scales are scrubbed away by high velocity gas flows, work by Man Labs Inc. has shown that some refractory diborides recede at 10 times the rate in furnace tests as compared to tests in a high velocity plasma. This is believed to be due to the effects of reaction time limitation and temperature gradients in a flowing environment.(4, Appendix F) In any event, this illustrative of experimental departure from intuitive expectation.

Materials For Short Term Use

For a lifetime less than 5 hours, reinforcing fibers of silicon carbide in a hafnium diboride matrix show some promise. This combination shows good strength and thermal shock resistance at room temperature but for all these systems there is a striking lack of fatigue data and most fracture toughness data are quoted only at room temperature. With these caveats, however, the SiC/HfB_2 system can withstand temperatures in excess of 2000 °C (3630 °F) for short periods of time.

Chemical Vapor Deposited (CVD) silicon nitride “has a chance” for surviving service at 3500 °F for 5 to 10 hours.(7) Si_3N_4 develops a protective coating of silica at high temperatures which limits oxidation. The CVD method of preparing the material avoids the formation of glassy boundaries which form between grains of material prepared by hot pressed sintering, thus crippling creep resistance of the material.

Outstanding properties of CVD silicon nitride include its hardness, high purity and resistance to chemical attack. The manufacturer, Praxair Surface Technologies Inc. (formerly Union Carbide Co.) recommends Si_3N_4 as a structural material for use in aggressive environments. Si_3N_4 evaporates at high temperatures. It has a vapor pressure of approximately 1 torr at 1450 °C (2640 °F).(8) No data are available on vapor pressure at temperatures significant to temperature sensor applications.

CVD deposit of Si_3N_4 creates a fairly rough, crystalline surface which must be ground smooth if required for a specific application. No information was obtained on fabrication techniques or capability for diffusion bonding. It may be possible to construct a male model of internal temperature sensor passages (mandrel) and deposit a closed Si_3N_4 structure around it to be removed by chemical means upon completion.

Despite extensive research work done over the past two decades, many deficiencies in the data exist. This can be seen in table 2, reproduced directly from reference 4. While this table nicely

TABLE 2 Comparison of Selected Ceramic Reinforcements and Composites

Materials	Flexure or Bend Strength (MPa) Room Temp	Flexure or Bend Strength (MPa) Elevated Temp	Creep @ 100 MPa (Sec^{-1})/Temp	Room Temp Fracture Toughness (MPa $\sqrt{\mu m}$)	Fatigue	Oxidation Resistance
Reinforcements						
Carbon	2000-4000	~2560 @ 2300°C	$1X10^{-11}$ @ 1600°C	U	U	Catastrophic
TiB_2/TiB(C)	670-1560	900 @ 1000°C	U	U	U	Poor
SiC (CVD)	-	1725 @ 1400°C	$3X10^{-9}$ @ 1600°C	U	U	Good
C-axis Al_2O_3	1400-3000	-	$1X10^{-8}$ @ 1600°C	U	U	Not Affected
C-axis BeO	-	~40 @ 1000°C	$1X10^{-9}$ @ 1750°C	U	U	Not Affected
YAG	U		$5X10^{-10}$ @ 1600°C	U	U	Not Affected
Non-Oxide/Non-Oxide						
BNp/AlN-SiC	-	28 @ 1530°C	U	U	U	Fair to 1600°C
SiC/SiC	350-750	-	U	18	U	$<10\mu m^2$/hr @ 1600°C
SiCp/HfB_2	380	28 @ 1600°C	$\sim 10^{-5}$ @ 1600°C	U (Good Thermal Shock)	U	12μm @ 2000°C
SiC_f/HfB_2-SiC	1000					5% wt gain @ 1600°C
SiC/$MoSi_2$	310	20 @ 1400°C	U	~8	U	$<10\mu m^2$/hr @ 1600°C
ZrB_{2pl}/ZrC(Zr)	1800-1900	U	U	18	U	Not known
20 v/o SiC_w/Si_3N_4	620	365 @ 1370°C	U	13	*	Good
Oxide/Oxide						
Al_2O_{3w}/Mullite	~180	-	U	U	U	Dissolution Reaction
Al_2O_3/ZrO_2	500-900	-	U	U	U	Not Affected
YAG/Al_2O_3	373	198 @ 1650°C	U	4	U	Not Affected
Non-oxide/Oxide						
SiC/ZrB_2-Y_2O_3	-	16 @ 1530°C	U	U	U	Poor
TiB_2/ZrO_2	U	U	U	U	U	Poor
SiC/Al_2O_3	600-800	U	10^{-5} @ 1525°C	5-9	U	Poor > 1200°C
30 v/oSic/ZrO_2	600	400 @ 1000°C	U	12	U	Degrades > 1000°C

U = Unknown
* = 0.2 μm crack growth after 500,000 cycles in compression @ 42 MPa

summarizes the properties of ceramic composites being considered for gas turbine applications, there are many important missing parameters as indicated by a “U.”

Refractory Metals

General properties of all potential materials for use in a temperature sensor and allied instrumentation considerations make cooling of the sensor imperative. After review of many exotic composites, the cooling requirement makes the higher thermal conductivity of metals an attractive option.

Molybdenum, tungsten, niobium, tantalum, rhenium and hafnium and their solid-solution alloys are most often mentioned in material literature. Each of these metals has its strengths and weaknesses, but some of the weaknesses can be overcome by alloying.

Tendency toward oxidation is an unfortunate weakness for all of them. For example, above about 1100 °C (2000 °F) molybdenum oxidizes to form MoO_3; niobium forms Nb_2O_5; and tantalum oxidizes rapidly to form Ta_2O_5. In addition, Nb_2O_5 is liquid above about 1450 °C (2600 °F). As a result, for use in a fluid temperature sensor application, refractory metals require protection unless the sensor structure is restrained to temperatures below their oxidation critical levels.

Tungsten has the highest melting point of any metal: 3410 °C (6170 °F) and is among the most dense. However, serious oxidation occurs above about 400–500 °C (750–930 °F). For temperature sensor fabrication, its high density and high thermal conductivity would aid in absorbing high temperature transients and moving thermal energy away from hot spots in the structure. Unalloyed tungsten is brittle at room temperature, but its ductility is improved by working and deforming. For example, a hot-worked tungsten bar is brittle at room temperature, but heavily worked tungsten wire is markedly more ductile.

The addition of rhenium to tungsten creates an alloy with significantly better ductility. W-Re alloys are significantly stronger than unalloyed tungsten. The rhenium also increases resistance to thermal shock and thermal fatigue. Unlike other alloys of tungsten, dispersion-strengthened W-Re alloys are only now nearing commercialization. The addition of hafnium carbide to the W-Re results in a material that is among the strongest ever produced for temperatures up to 2000 °C (3630 °F).

Thoriated tungsten, dispersion-strengthened with ThO_2, increases the high temperature strength of unalloyed tungsten resulting in a maximum temperature capability several hundred degrees higher. Thoriated tungsten is commercially available. It is used for forged valve bodies in spacecraft attitude control systems and other high-temperature aerospace components.

Tantalum is the most corrosion resistant of the refractory metals at moderate temperatures (about 150 °C or 300 °F). This corrosion resistance results from the formation of a thin oxide coating, which, because it is relatively thin, is a suitable heat transfer surface. However, it cannot be used at temperatures above about 260 °C (500 °F) in an oxidizing atmosphere without a protective coating. Its heat transfer coefficient ranges from about 1/3 to 1/2 that of tungsten at temperatures up to 2527 °C (4580 °F).

Lockheed Missiles and Space Co. Inc. reports successful use of niobium and tantalum alloys at 1600 °C (2900 °F) using a silicide protective coating.(9) Niobium C103, composed of niobium, 10% hafnium, and 1% titanium, will function at 1600 °C and is capable of diffusion bonding. The silicide coating was reported as competent in the presence of thermal cycling.

Silicide coatings encounter the same problems described in the discussions of carbon/carbon protective systems. Defects in the coating allow infiltration of oxygen to the metal substrate. The most significant defects in the silicide coatings result from fissures formed during thermal cycling due to the mismatch of the coefficient of thermal expansion. While the coating lifetime is reported to be in the hundreds of hours, up to temperatures of 1500 °C (2700 °F), expected service is "substantially less" in the presence of thermal cycling.(10)

PRESSURE TRANSDUCERS

In the 25 years since the original NASA fluid temperature sensor program, pressure transducer technology has advanced in some ways but not in directions which enhance use as a temperature sensor read-out device. The Kistler organization has eliminated the 601L transducer, used on previous sensors, from its line of standard products. Its 540 °C (1000 °F) ambient capability has been replaced by a device limited to 260 °C (500 °F). Other manufacturers of piezoelectric transducers, by using miniature integrated circuits, have incorporated the amplifier electronics into the transducer body itself. This limits the environmental temperature of the transducer to the temperature capability of the solid state electronic components rather than the limit imposed by the quartz piezoelectric element.

A new piezoelectric material has appeared which has a Curie temperature greater than 600 °C (1112 °F). This product, manufactured by Keramos Inc., is designated Käzite K15 and is a piezoelectric ceramic. Keramos does not manufacturer pressure transducers, only the raw ceramic material. In our search for high temperature, high frequency transducers, we encountered a manufacturer of high power, driver transducers which convert an electric signal into mechanical motion, but no pressure transducer manufacturers using the Käzite piezoceramic.

Piezoelectric Transducers

In general, piezoelectric transducers still hold the most promise for temperature sensor applications. The Kistler devices as used on the earlier program are still a nominally good solution. New piezoelectric transducer suppliers have evolved and show more enthusiasm for working "special problems" than "everything-we-have-is-in-our-catalog" attitude that has sometimes prevailed in the past.

Potential Suppliers and Products

	Kistler Instrument Corp.	PCB Piezotronics Inc.
	Model 6001	Model 105B02
Threshold psi	0.03	0.005
Pressure range psi	3,600	250
Natural frequency	150 KHz	250 KHz
Temperature range	–195 to +350 °C	–100 to +250 °F
Diameter	0.219 in.	0.099 in.
Length	0.58 in.	0.81 in.

The PCB device fits inside the diameter of a 10-32 screw (root diameter 0.140").

Solid State Transducers

Solid state devices, primarily strain gauge bridge networks directly deposited on a silicon substrate, have been highly developed. The resistance legs are laser trimmed to produce required design characteristics and temperature compensation circuits are deposited on the chip along with the bridge resistors. Unfortunately, most of these devices appear to have resonant natural frequencies of approximately 35–40 KHz. Based on data from reference 11, a fluid temperature sensor at 10,000 °R would be expected to have an output frequency of just over 100 KHz and even at 2000 °R, the output frequency is about 45 KHz. This characteristic alone would limit the usefulness of the solid state devices, found in our search, to temperatures below about 1000 °R.

The Entran Corporation (Appendix C) produces (by special order) a small (0.14" diameter) silicon device, protected with a stainless steel diaphragm, which can function at 500 °F. From a resonant frequency standpoint this device would be useful to approximately 3000 °F and is worthy of consideration for lower temperature operation simply because of its small size.

ANALYTICAL TIME RESPONSE STUDIES

Time Response

A major objective of this program is to drive the measurement capability of the acoustic sensor as far as possible toward a 5540 °C (10,000 °F). Since one of the more attractive features of this technique is its rapid time response, a short study was made of the effect of temperature, pressure and various gases and gas compositions on sensor time response.

Acoustic sensor time response has two components:

1. An initial, flow-induced response related to the “flushing time” of the sensor cavity. This is the time required for the fluid in the sensor to be replaced by a mass of fluid at a new temperature and is in the millisecond range.

2. A sensor body mass time constant, which is a function not only of the flow through the sensor, but also the sensor mass and thermal conductivity of the material, the flow field around the sensor exterior, heat transfer characteristics of the internal and external flow geometry and the cooling means used to allow the device to survive extremely high temperatures.

Analytically these two components of the time response can be represented by the following equation taken from reference 11:

$$\frac{T_m - T_o}{T_{in} - T_o} = 1 - C_1 * e^{-t/\tau} - C_2 * e^{-t/\tau}$$

where: T_m = Temperature of fluid inside sensor
T_o = Initial temperature of body and fluid
T_{in} = Temperature of fluid to be measured (step change from T_o)
C_1 = $K_1/(K_1 + K_2)$
C_2 = $K_2/(K_1 + K_2)$
K_1 = $c_p m_f / c_v m_f$

K_2 = $hA_Q/c_v m_f$
t = time
τ_1 = $1/(K_1 + K_2)$
τ_2 = $(K_1 + K_2)/(K_1 K_3)$
K_3 = $hA_Q/c_B m_B$
h = convective heat transfer coefficient
c_B = specific heat of sensor body material
m_B = mass of sensor body

The first term of the equation can be quite easily computed if the mass flow rate through the sensor is known. The second term, representing the body heating rate is much more difficult to estimate. After a change in temperature, the body comes to some new temperature much more slowly than the gas in the sensor cavities. The body is heated, not only by the internal flow in the cavities, but also by external flow around the sensor body. The new equilibrium must include radiation losses from the sensor body to any radiation shield and is also influenced by the flow through the radiation shield.

At very high temperatures, the body temperature must be controlled to approximately 80% of the melting temperature of the body material. Thus, above some material-dependent temperature, the body temperature must be held constant by some liquid or cryogenic cooling means and the time variable effect of body mass heating is negligible. However, the temperature gradient between the sensor body and the mass of the fluid in the acoustic cavity would be limited to the boundary layer. It may be necessary to remove the boundary-layer bias from the measured fluid temperature by measuring the controlled body temperature and measure the bias with a calibration process.

The sensor time response was computed using a truncated version of equation (10) from reference 11, eliminating the third term which deals with the secondary body heating/cooling effects:

$$\frac{T_m - T_o}{T_{in} - T_o} = 1 - C_1 * e^{-t/\tau}$$

However, rather than using constant values for the specific heats of the gas in the sensor, the specific heats were adjusted to account for changes with temperature.

Reference 1 gives tabular values for the specific heats of air and combustion products. They range from 100–6400 °R for air and from 300–4000 °R for 400% theoretical air combustion products. As in the Knudsen number analysis, regression analysis was again used to determine the specific heats.

All other variables in the equation were formulated in terms of pressure and temperature so that the effects of these environmental variables could be quickly assessed. Gas density and mass flow were computed using the equation of state. The flow through the sensor was derived from the calibration data shown in the following figure (fig. 6), reproduced from figure 12 of reference 11.

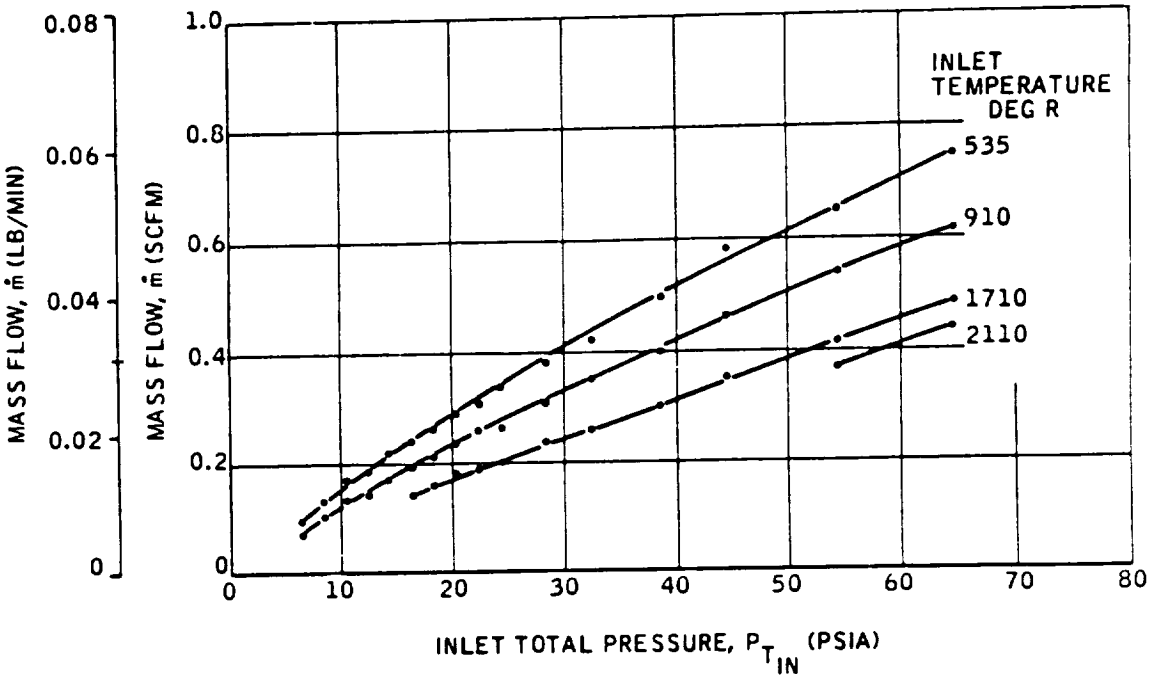

Figure 6: Flow Calibration of Fluid Temperature Sensor

The data in this plot were subjected to a second-order multiple regression giving the following relationship. This equation reproduces the data to a standard deviation of about 7 parts in 1000 (0.7%). Mass flow through the sensor in lb./sec. is given by:

$$m_f = 0.0765\,(6.16181\text{E}{-}03 + (2.16252\,p) - (1.1251\text{E}{-}04\,p^2)\,(-4.9695\text{E}{-}06\,T) + (1.2752\text{E}{-}09\,T^2) - (1.3823\text{E}{-}05\,p\,T)\,(+1.162\text{E}{-}07\,p^2\,T) + (3.8\text{E}{-}09\,p\,T^2) - (3.919\text{E}{-}11\,T^2))/60$$

The internal volume and surface areas of the sensor were estimated from the drawings included in reference 11. The heat transfer coefficient range for forced convection, turbulent flow was taken from Table XI, Chapter VIII of reference 1. From the spread sheet data four plots of sensor time response were made:

1. Figure 7: Air at constant pressure with temperature varying from standard conditions to 6,400 °R.

2. Figure 8: Air a constant temperature with pressure varying from standard conditions to 65 psia, the highest pressure for the sensor mass flow data included in reference 11.

3. Figure 9: Air at standard conditions with variable heat transfer coefficient.

4. Figure 10: Air, 400% theoretical combustion products and argon at 40 psia and 910 ° R.

Inspection of these plots shows that, for a sensor with a controlled body temperature, increasing air temperature results in an improved sensor time response, figure 7. The higher temperature results in a higher velocity through choked-flow sections of the sensor allowing a more rapid replacement of the fluid in the sensor body. It should be noted that this is opposite the result expected for a passive, uncooled sensor where the body mass must be brought to a new temperature by both the

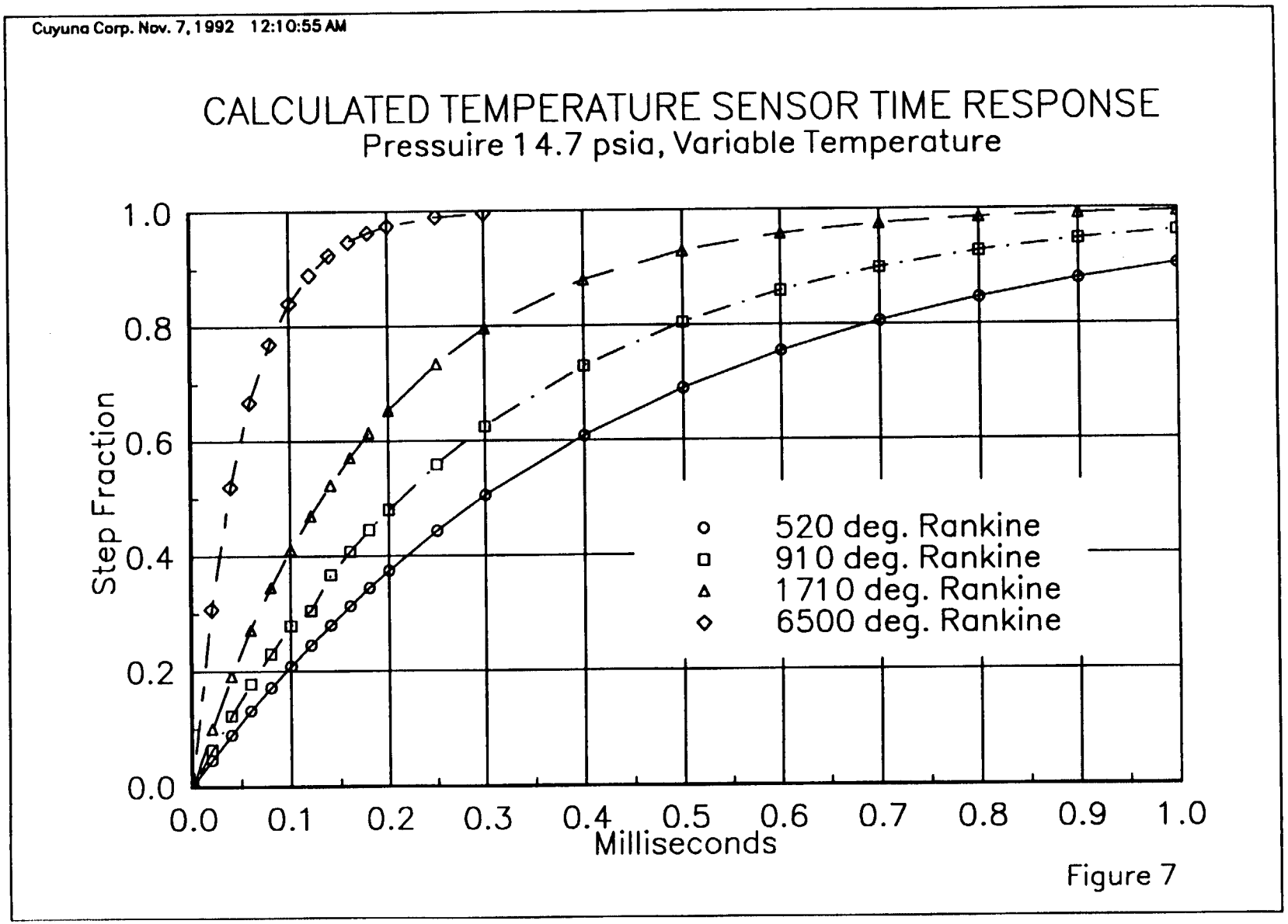
Cuyuna Corp. Nov. 7, 1992 12:10:55 AM
CALCULATED TEMPERATURE SENSOR TIME RESPONSE
Pressuire 14.7 psia, Variable Temperature
Step Fraction
1.0
0.8
0.6
0.4
0.2
0.0
0.0 0.1 0.2 0.3 0.4 0.5 0.6 0.7 0.8 0.9 1.0
Milliseconds
520 deg. Rankine
910 deg. Rankine
1710 deg. Rankine
6500 deg. Rankine

Figure 7

interior flow and exterior flow around the sensor. For this condition, the lower density of the higher temperature flow results in a decreased ability to transfer heat to or from the sensor body.

Pressure effects tend to lengthen the time response of the sensor but not significantly for the range of pressure studied, figure 8. Again, this is the result for a sensor with a cooled body. For a passive sensor, one without controlled body temperature, the increased pressure would increase gas density and tend to improve the time response.

Varying the heat transfer coefficient by a factor of 5 shows a negligible effect. In a passive sensor, time response would be expected to be approximately proportional to the heat transfer coefficient. The results shown in figure 9 occur only because no attempts are being made to change the sensor body to a new temperature.

Finally, figure 10 shows the results for different gases at 40 psia and 910 °R which is in the range of gas turbine exhaust temperatures. As expected, there is little difference between air and the 400% theoretical air combustion products. Argon is included to compare the results for monatomic with those for air.

Dissociation Effects

A limited effort was made to determine the effect of dissociation on temperature sensor performance. The frequency of temperature sensor oscillation is a function of the speed of sound of the gas within the instrument cavity. The speed of sound is, in turn, a function of the square root of the absolute temperature of the gas. For past sensor configurations the temperature/frequency relationship has ranged slightly, around the square root, i.e.,

$$T = K_1 f^{1.867}$$

to

$$T = K_2 f^{2.0855}$$

To explore effects which might be due to dissociation, the speed of sound was computed with γ = constant = 1.4 and with γ calculated from the C_p/C_v with the temperature relationship as defined in the section on Knudsen number. The specific heat values were determined for absolute temperatures ranging between 500° to 6400°, the highest values listed in reference 1. The results are shown in figure 11. At 6400° the speed of sound computed by the two methods differs by about 3.5%. As the plot shows, the speed of sound relationship with temperature and with temperature varying γ shows slightly more curvature (power relationship slightly greater than 2). However the relationship with γ computed, γ_c:

$$\text{Value}/1000 = K\gamma_c \; 1716 \; T$$

is linear, despite the nonlinear relationship of C_p and C_v with temperature. K has been chosen arbitrarily to make the value fit the chart.

In any event, none of the relationships show any breaks in curvature which might indicate dissociative effects. The air data in reference 1 may not be carried to a sufficiently high temperature or may simply need updating to include current experimental findings. The regularity and linearity of the curves might mean that the tables of reference 1 are analytically determined and, as a result, may not show real gas effects. This area needs further exploration using better data showing dissociation effects.

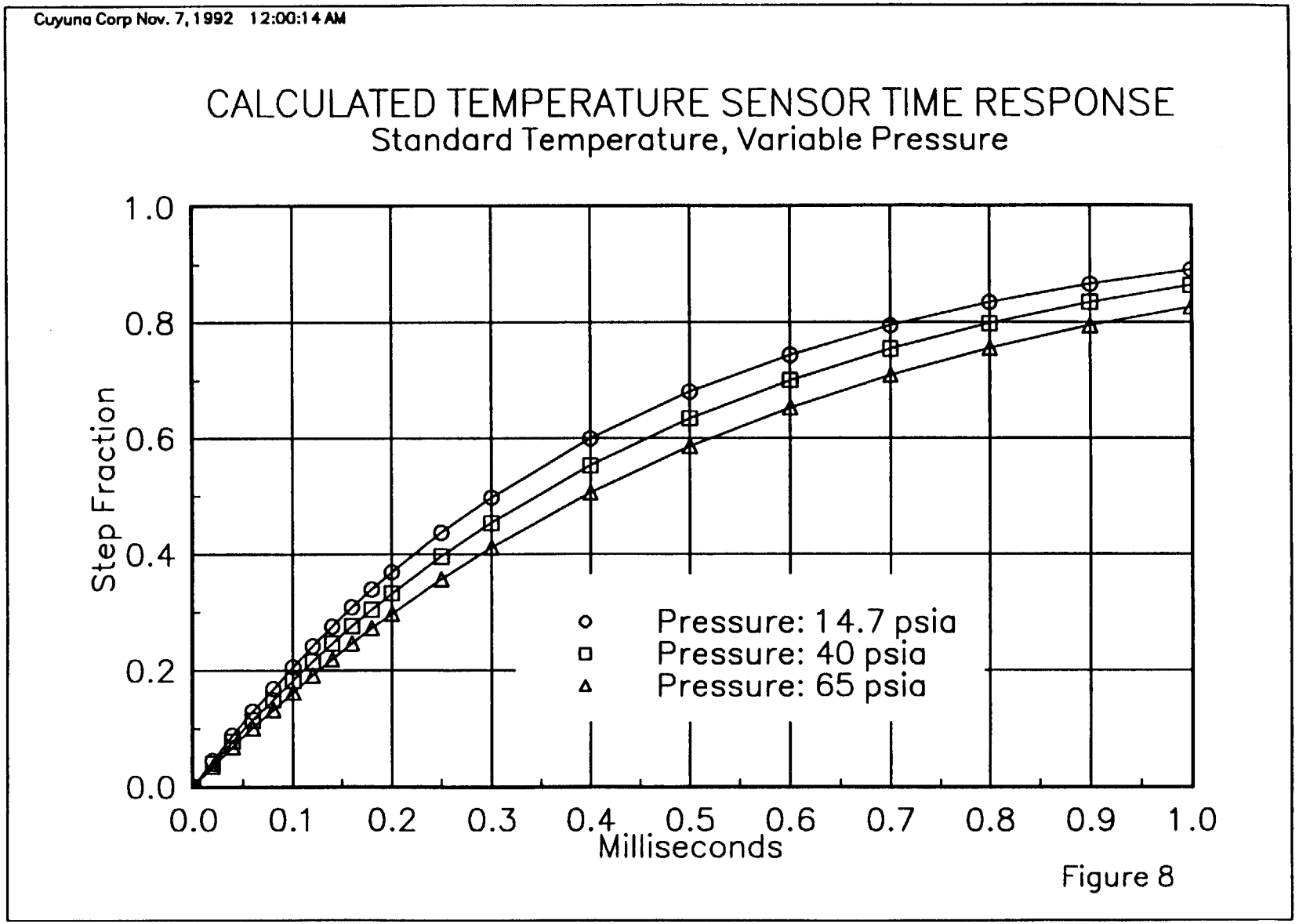
Cuyuna Corp Nov. 7, 1992 12:00:14 AM
CALCULATED TEMPERATURE SENSOR TIME RESPONSE
Standard Temperature, Variable Pressure
Step Fraction
1.0
0.8
0.6
0.4
0.2
0.0
0.0 0.1 0.2 0.3 0.4 0.5 0.6 0.7 0.8 0.9 1.0
Milliseconds
Pressure: 14.7 psia
Pressure: 40 psia
Pressure: 65 psia

Figure 8

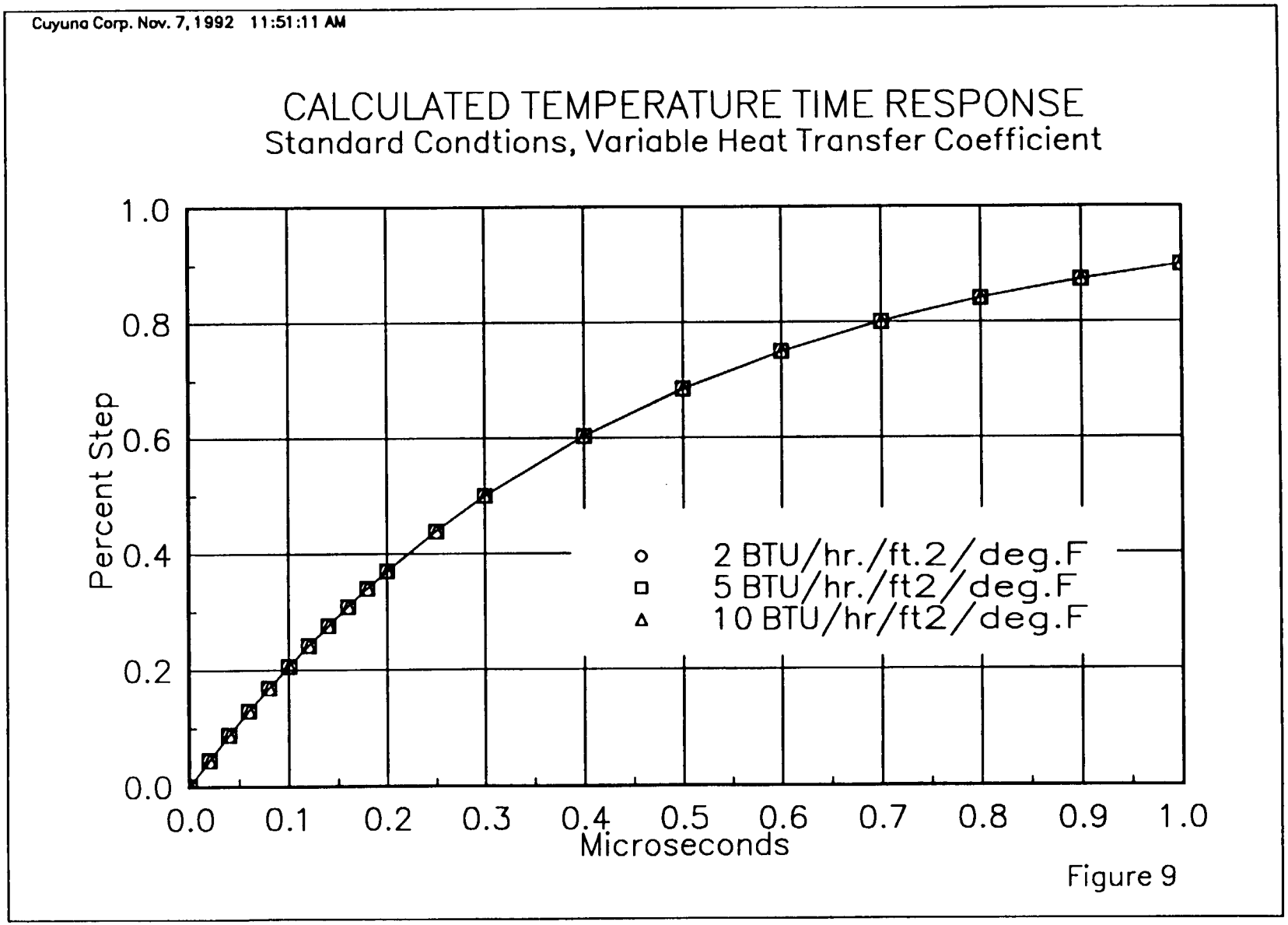
Cuyuna Corp. Nov. 7, 1992 11:51:11 AM
CALCULATED TEMPERATURE TIME RESPONSE
Standard Condtions, Variable Heat Transfer Coefficient
Percent Step
1.0
0.8
0.6
0.4
0.2
0.0
0.0 0.1 0.2 0.3 0.4 0.5 0.6 0.7 0.8 0.9 1.0
Microseconds
2 BTU/hr./ft.2/deg.F
5 BTU/hr./ft2/deg.F
10 BTU/hr/ft2/deg.F

Figure 9

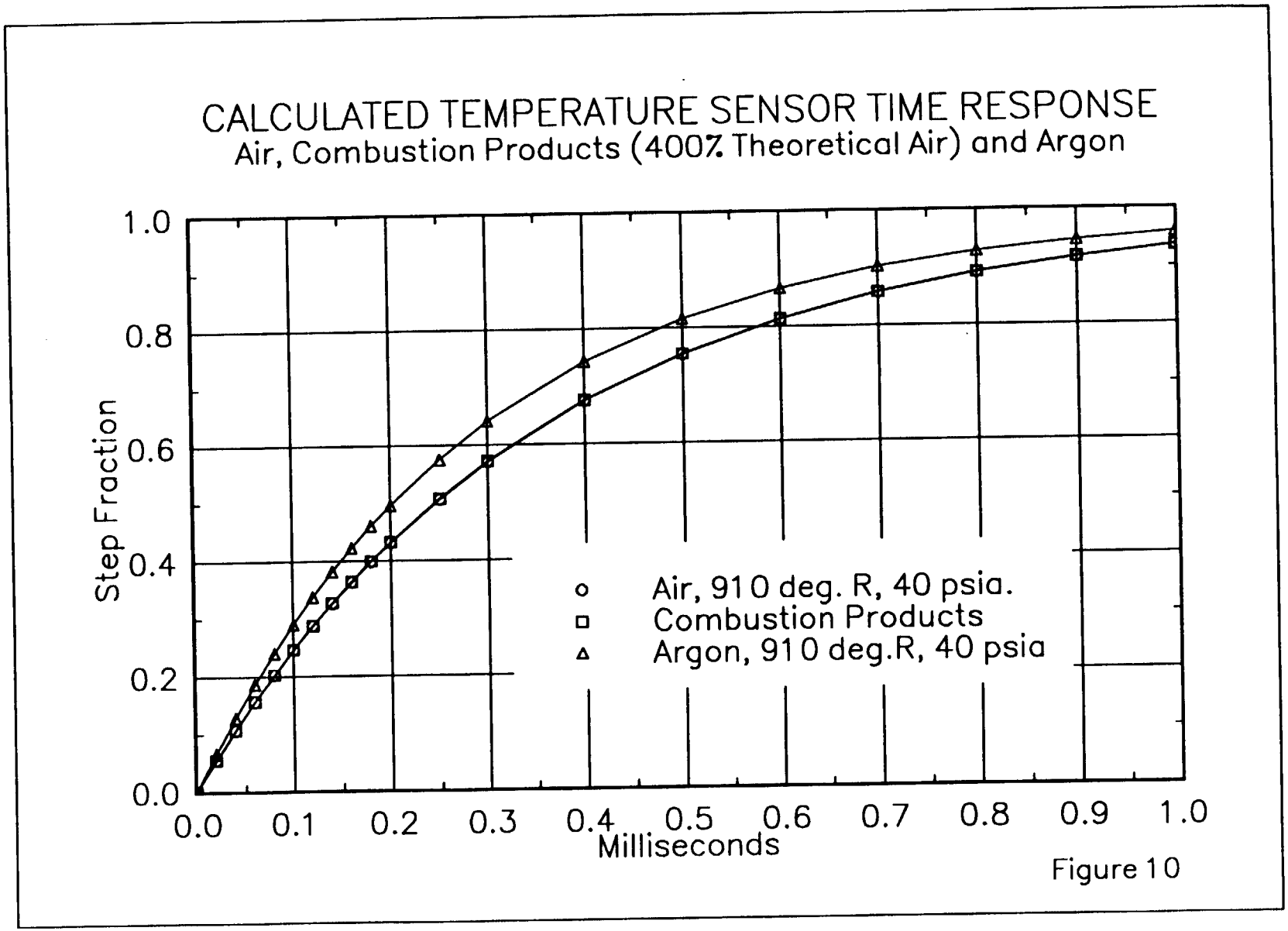
CALCULATED TEMPERATURE SENSOR TIME RESPONSE
Air, Combustion Products (400% Theoretical Air) and Argon
Step Fraction
1.0
0.8
0.6
0.4
0.2
0.0
0.0
0.1
0.2
0.3
0.4
0.5
0.6
0.7
0.8
0.9
1.0
Milliseconds
Air, 910 deg. R, 40 psia.
Combustion Products
Argon, 910 deg.R, 40 psia

Figure 10

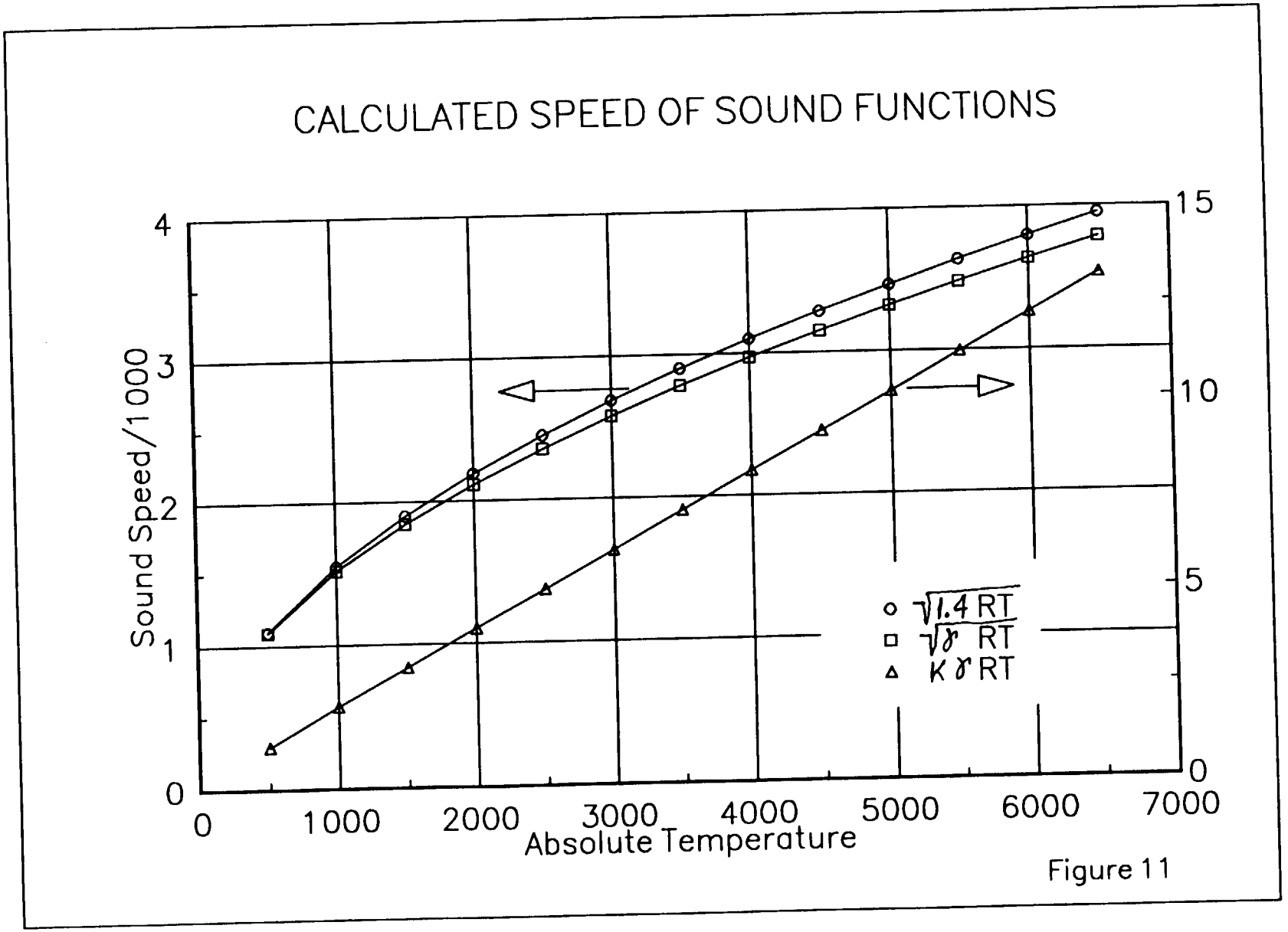
CALCULATED SPEED OF SOUND FUNCTIONS
Sound Speed/1000
Absolute Temperature
0
1000
2000
3000
4000
5000
6000
7000
1
2
3
4
5
10
15
$\sqrt{1.4\,RT}$
$\sqrt{\gamma\,RT}$
$K\gamma RT$

Figure 11

FABRICATION CAPABILITIES

As stated in our proposal, Cuyuna Corporation has only limited capability for fabricating experimental sensors and supporting laboratory equipment. One item of the contract work statement calls for exploring various means for building temperature sensor hardware. Five avenues were surveyed: A major space equipment manufacturer A manufacturer of total temperature sensors for aircraft, A manufacturer of flow research instrumentation, A small engineering firm, An aeronautical instrument manufacturer. Formal presentations and subsequent discussions were held with three of these organizations; one was contacted by telephone, and information was exchanged by telefax and mail with one firm, located in England.

Lockheed Missiles and Space Co. Inc.

Telephone discussions were held with Dr. Jerry P. Wittenauer a Research Scientist with Lockheed. He expressed an interest in working with Cuyuna in the development of applications for Lockheed's high temperature materials. He stated that he has IR & D funds designated for this type of activity in 1993. These funds could be applied in concert with future contract funding by supporting work in specific problem areas related to temperature sensor fabrication. Wittenauer later confirmed Lockheed's interest in writing.

Rosemount Inc., Aerospace Division

Rosemount Inc. was founded in 1956 by a group of scientists working at the Aeronautical Research Laboratories of the University of Minnesota. The company's initial product was a temperature sensor designed to accurately measure total temperature over a wide range of flight conditions. Since that time Rosemount has expanded its range of products to include:

Pitot-static pressure
Flow angle
Angle of attack
Ice detection
Fuel and oil temperature
Engine inlet pressure and temperature
Cryogenic and surface temperature for space craft
Complete air data systems

Rosemount sensors now provided air data for most commercial and military jet aircraft worldwide.

A formal presentation was made to Mr. Donald Thompson, Director of Temperature Operations for Rosemount Aerospace Division and several of his technical staff. Following a period of evaluation Cuyuna was notified in writing that Rosemount would be willing to support Cuyuna's hypersonic temperature sensor development. It will be necessary to develop a Statement of Work defining the effort required of Rosemount and a working agreement between Cuyuna and Rosemount.

Successful completion of these documents will provide NASA and Cuyuna access to all the fabrication and laboratory facilities essential to proceeding beyond the current phase of the temperature sensor program.

Schlumberger Industries Aerospace Division

Schlumberger Aerospace is an agglomeration of several instrumentation companies, including Farnbourough Transducers, Weston Instruments, assembled to lend size and credibility for dealing with major aircraft manufacturers. Several of these organizations have been relocated to Farnbourough, England and placed under unified management. As a result of the contract notice for the current contract, published in the Commerce Business Daily, we were contacted by JGW International a Washington, DC firm representing Schlumberger Aerospace Division. Initial contact sought to purchase Cuyuna's instrumentation products. When it was explained that no products were currently being manufactured, succeeding contacts began to explore acquiring the technology. Information and data from the old Honeywell reports were sent to Schlumberger and contact continues at a relaxed level. The capability of Schlumberger Farnbourough to support a temperature sensor development program has not been assessed.

TSI Incorporated

A formal presentation was made to TSI Incorporated represented by:

Dr. Leroy M Fingerson, President and CEO
Mr. Gregory Vack, General Manager
Dr. Rajan Menon, Principal Engineer
Mr. Ralph Kiland, Principal Engineer

TSI Incorporated is a worldwide supplier of flow-oriented instrumentation for research and industry. It was founded in 1961 and is headquartered in St. Paul, Minnesota with subsidiaries in Sunnyvale, California and Germany. The principals of TSI and Cuyuna Corporation have shared professional working relationships for over 25 years.

TSI's origins lie in hot wire instrumentation for aerodynamic and other flow research. The company now designs and manufactures sensors and instrumentation systems for:

Velocity, flow and other characteristics of fluids
Small particles suspended in fluids (contamination or pollution)
Meteorological measurements (atmospheric and environmental)

TSI's expertise includes laser light scattering techniques including laser velocimetery, fiber optics, high speed electronics, complex sensor fabrication and specialized software. TSI was chosen because one of its focal markets is the research community: universities, government (including NASA) and industrial laboratories are among its customers. The company's staff is thoroughly familiar with building research instrumentation in small quantities for specialized needs.

After several weeks of internal evaluation, TSI has informed us that it cannot support Cuyuna Corporation's development of an improved hypersonic temperature sensor. Several years ago, TSI embarked on an aggressive market diversification program and is reluctant to divert from its chosen development areas to undertake an additional technical area.

Volna Engineering Inc.

Several formal discussions were held with Mr. William Volna, President of Volna Engineering. Volna Engineering is a small, highly technical development shop run by a graduate mechanical

engineer. For more than twenty years, Volna has built solar trackers, precision instrumentation and specialized test equipment for DOD and industrial users under sub-contracts from a variety of prime contractors. The company has broad capability for fabricating parts and equipment using conventional machining methods. It would be ideally suited to build experimental temperature sensors.

Volna's main disadvantage is its limited availability due to current workload. The company's capabilities are vested in its President and owner and are not easily multiplied to the same high order skills displayed in past projects.

CONCLUSIONS

Pressure Transducers

Transducer technology has not advanced relative to high temperature capability. Effective cooling will be required to get information out of the sensor via pressure sensing techniques. As a result, all the difficult design compromises of the earlier programs persist. In essence, this means balancing signal pulse strength, pressure port length, transducer sensitivity and transducer cooling details. It may be possible to take quick, short-term measurements using a simple, uncooled sensor built from a heavy, high-heat-capacity material. For long-term measurements, cooling the transducer area will be essential.

Materials

Material developments have not advanced high-temperature materials to a level which will permit the fabrication of an fluid temperature sensor whose oscillation cavity operates at 5,500 °C (10,000 °F) without cooling. It may be possible to build a simple, uncooled oscillator cavity for long term operation up to 1650 °C (3000 °F). For 5–10 hour life in a cycling environment some materials may allow use of an uncooled cavity to temperatures of approximately 1900–2200 °C (3500–4000 °F). As discussed above, it would still be necessary to strategically locate the pressure transducer or cool it, or both.

For measurements to 10,000 °F, designs based on refractory metals, having reasonable oxidation resistance, should be explored. Since both the pressure transducer and the temperature sensor body must be cooled at the higher temperatures, consideration should be given to holding the entire system below the oxidation temperature of the sensor material. Because the sensor internal design involves stagnation of the flow at some points, the development of “hot spots” is a real threat to long life of the sensor cavity. The high thermal conductivity of metals compared to that of most ceramics should aid in relieving the tendency to concentrate heat at discrete points.

No thermodynamic design studies were conducted, but efficient cooling of the oscillator cavity may offer the best hope for an ultra-high-temperature sensor based on fluid techniques. Such a design would involve a network of cooling passages with liquid or cryogenic gases flowing through the body structure. The coolant would be discharged overboard, downstream of the inlet port, so as to not affect the measurement by foreign gas contamination.

Rarefied Gas Effects

For use in the flight environment, rarefied gas effects are less severe than expected in the high Mach numbers. Analysis of the Knudsen number behavior showed that the worst effects (approach to

slip-flow) occurred at Mach = 1. At higher Mach numbers, the stronger shocks resulted in lower velocities behind the shock and combined with other effects, maintained a nearly constant Reynolds number component of the Knudsen number.

Fabrication Capability

Cuyuna's limited facilities require augmentation to fabricate and test developmental temperature sensors. This can be accomplished either by internal enhancement or joining with a company having the needed facilities. A variety of potential joint venture candidates were surveyed to determine interest and capability. Candidates ranged from a small developmental engineering company to a major aerospace firm. Two written expressions of interest in participation were received one from Rosemount Incorporated and one from Lockheed Missiles and Space Co. Inc.

APPENDIX A

A Short History of Fluid Temperature Sensors

Early Work

The fluid amplifier concept originated at the Army's Harry Diamond Laboratories in the early 1960s and by 1964 a variety of concepts and configurations had evolved. The Laboratory's work included some of the earliest known work on the use of fluid oscillator concepts for measuring temperature. References 1 and 2 cite temperature measuring work dating to 1964 and 1965.

Honeywell Developments

In 1960 Honeywell purchased licenses to fluid amplifier technology and started a fluid mechanic laboratory to research the basic operating principles of these devices and to develop products incorporating air and liquids as the working medium. One of the areas of focus was the temperature oscillator.

By 1964, under the contractual sponsorship of the Aero Propulsion Laboratory of Wright Patterson Air Force Base, Honeywell's temperature sensor work had progressed to the point where a temperature oscillator was incorporated into the primary control loop of a General Electric J85-5 jet engine.

In other areas, Honeywell developed a fluid angular rate sensor, which had no moving parts. In 1963, combined with other fluid amplification devices, the fluid rate sensor was the heart of a control system used to fly a demonstration missile flight with compressed air as the working medium and no electronics. This program was sponsored by the Army. The fluid rate sensor operating on oil was also used in a hydraulic, single axis rate damping system for helicopters. In general, the driving force behind this technology was simplicity, high temperature environment and immunity to the nuclear electromagnetic pulse.

NASA Sponsored Work

In 1965 NASA Ames Laboratory contracted with Honeywell for a series of research programs to explore the potential of fluid oscillators for temperature sensing in various hypersonic wind tunnel applications. The Air Force sponsored work for jet engine measurements had resulted in relatively large devices. Because one of NASA's prime interests was in boundary layer measurements, the work concentrated on miniaturization.

Earlier work was used as a starting point but the difficulties of small size soon became apparent:

* Viscous losses in small passages attenuated the magnitude of the pressure pulses

* Signal wave forms were distorted and dominated by noise at higher total pressure levels
* Machining tolerances became critical and surface finishes better than 15 microinches were required on all internal flow passages
* Diffusion bonding became the only feasible means of assembly so this imposed another overriding requirement on material selection in addition to the already severe environmental requirements. At these temperatures, adhesives were out of the question and welding introduced undesirable thermal stresses in relatively brittle materials. Ultimately these problem areas were overcome with engineering compromises which resulted in a number of successful instruments.

Three temperature probes delivered under the contract; two "low temperature" (temperatures to 2300 deg. R), designated Probe A and B, and a high temperature version capable of operation at 3500 deg. R. The low temperature probes are shown in figure A-1 (Probe A) and figure A-2 (Probe B). The two low temperature probes had the same internal oscillator configuration figure A-3, except for the signal tube exit which had to conform to either a straight or a swept back pylon. The high temperature probe is shown in figure A-4 along with it's internal dimensions figure A-5.

Geometric Compromise

The probe internal geometry was developed using a a variable geometry model which could be clamped together for rapid configuration changes. Selection of the optimum exit orifice location was dictated by signal waveform shape and signal-to-noise ratio which are major indicators of oscillatior performance. Exit orifice size and location coupled with transducer sensitivity and location were the prime parameters investigated. They were investigated over a wide range of inlet pressures.

While some research measurements showed that oscillation could be maintained down to absolute pressures of 0.1 psia the practical lower limit for these wind tunnel applications was about 1.0 psia. Transducer sensitivity available in 1967 resulted in a capability to detect oscillations at 4.5 psia for Probe A and to 1.3 psia for Probe B. A typical characteristic plot, taken from a Probe B configuration, is shown in figure A-6.

Final configurations resulted from a balancing of thermal, mechanical and pressure measurement considerations. In general, more sensitive pressure transducers also exhibit temperature interactions so must be cooled and/or located farther from the oscillator. Internal passage length attenuates the pressure signal, limiting the distance the transducer between the transducer and oscillator. Smaller oscillators give lower pressure pulses, simply because there is less total energy in the flow. Transducer developments since the mid 1960s might change the design optimizations and result in temperature sensors with better performance and extended range of operation.

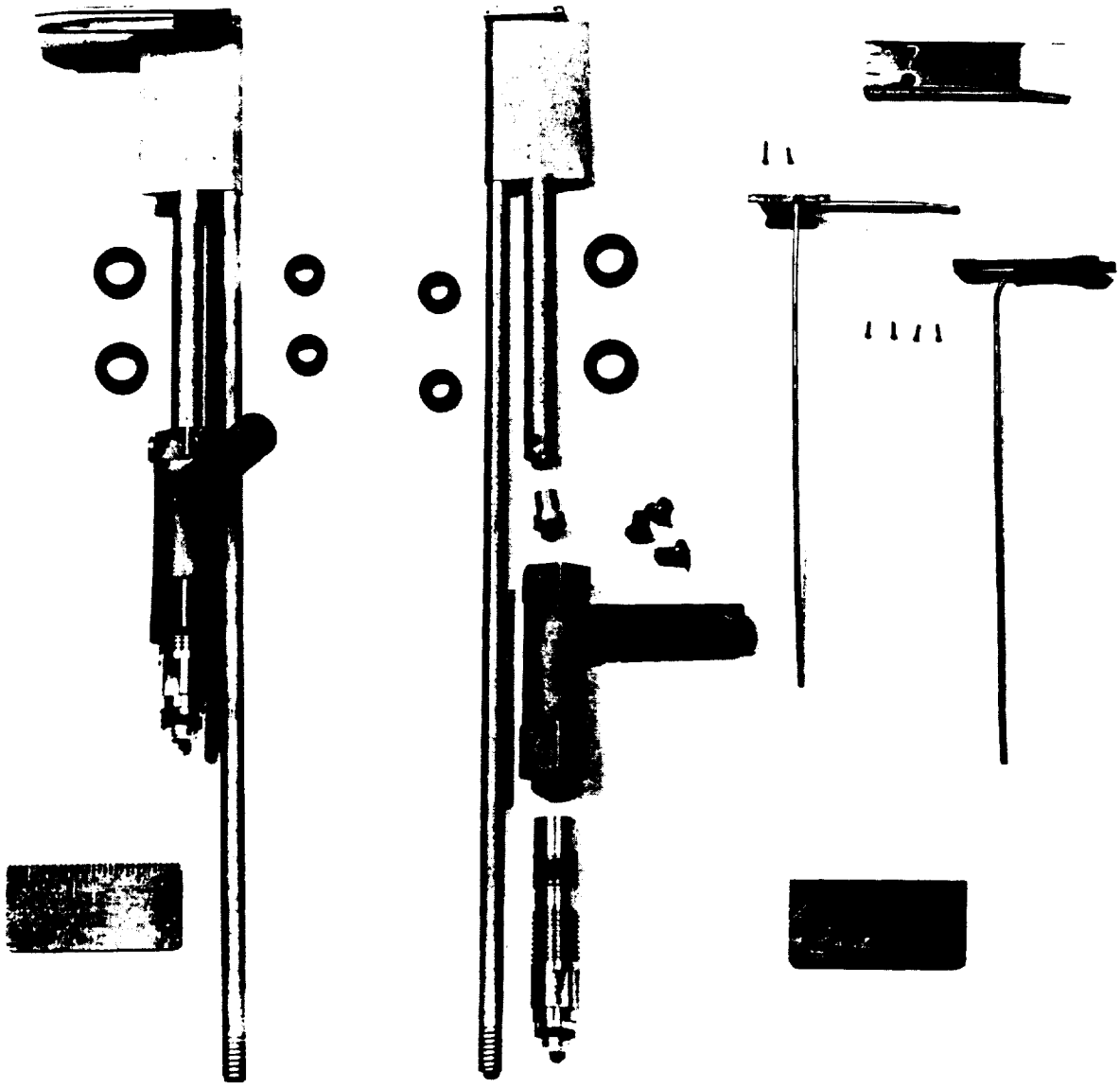

Low Temperature Probe A, Assembled and Disassembled

Figure A-1

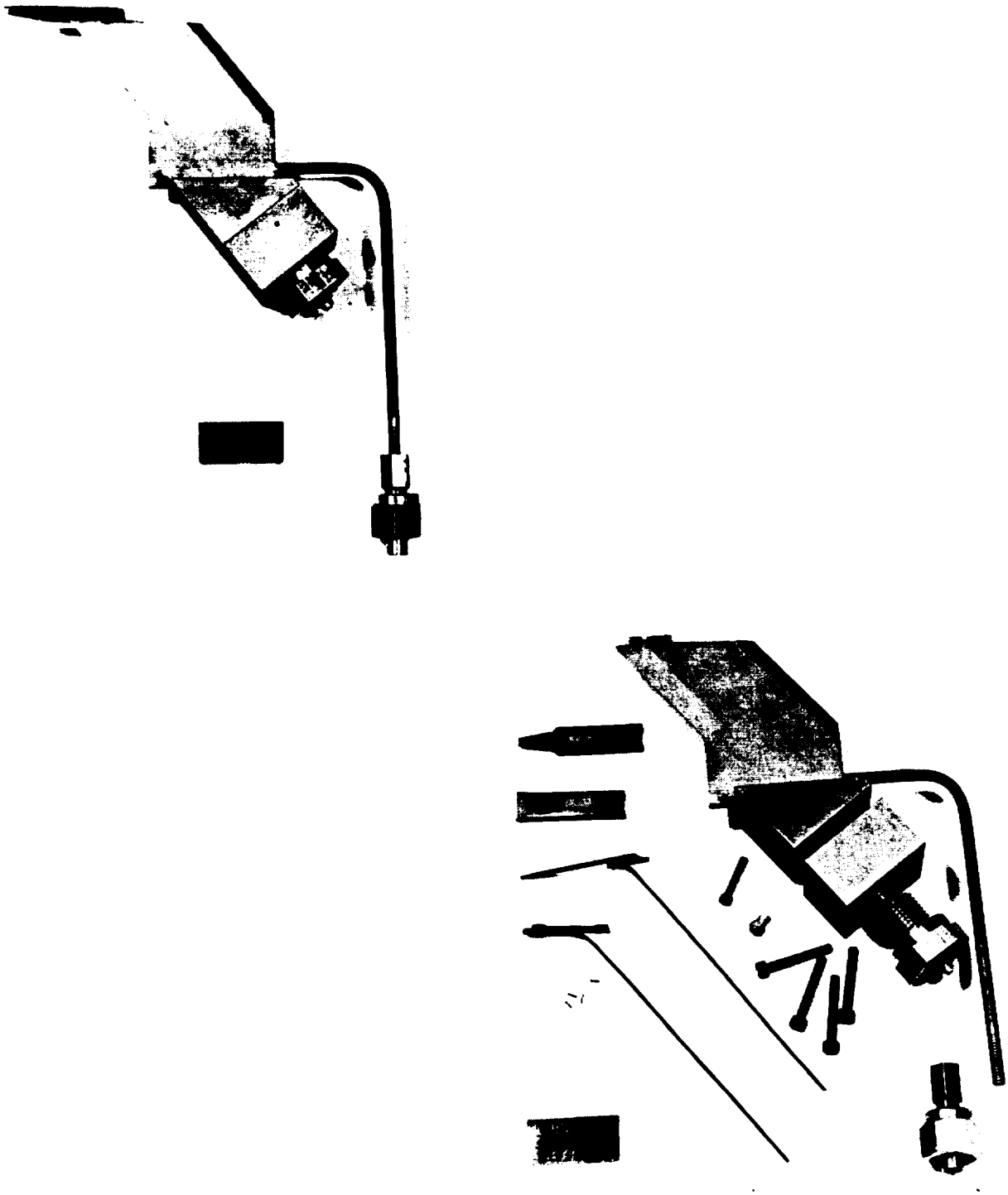

Low Temperature Probe B, Assembled and Disassembled

Figure A-2

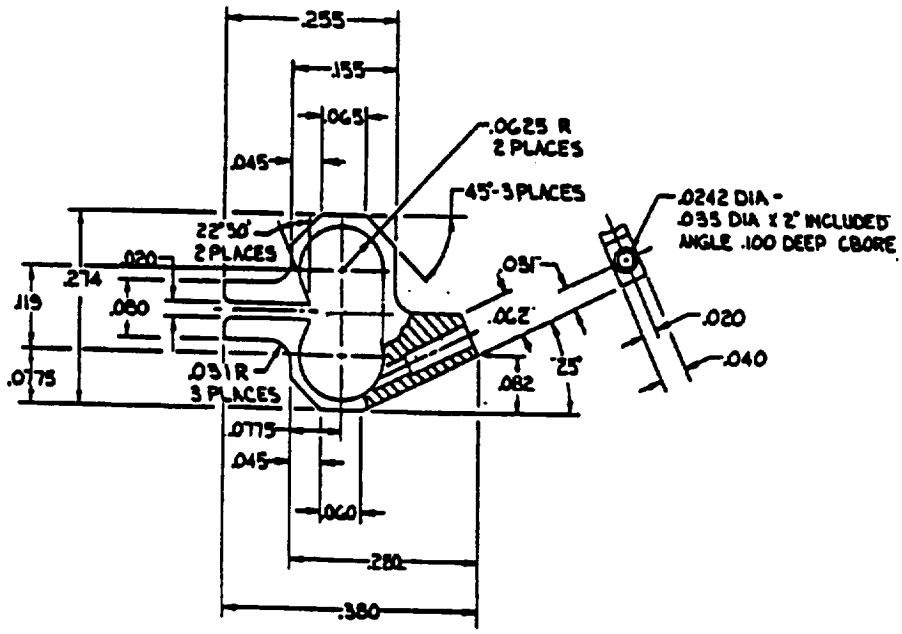

Internal Geometry, Low Temperature Probes A and B
Figure A-3

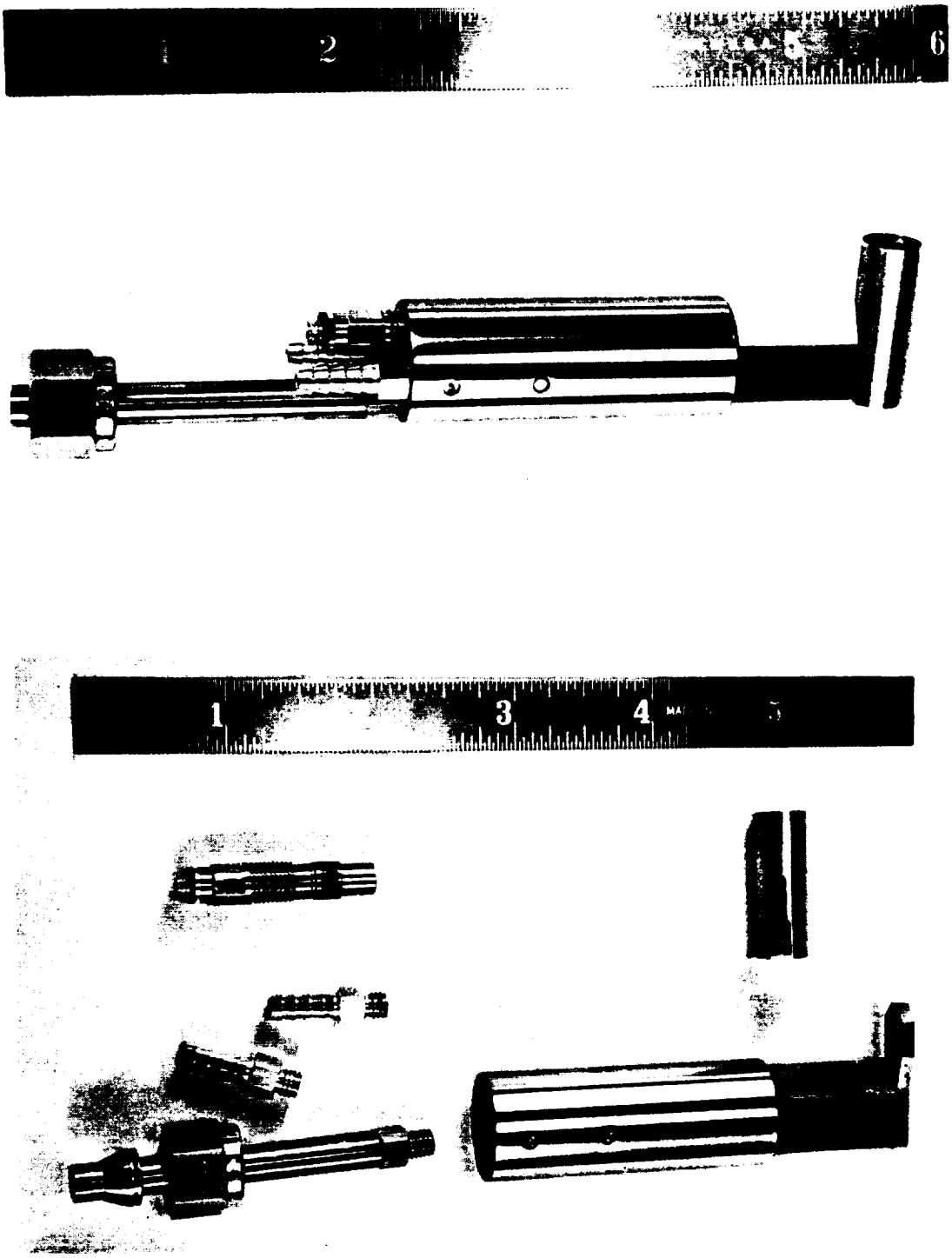

High Temperature Probe C, Assembled and Disassembled

Figure A-4

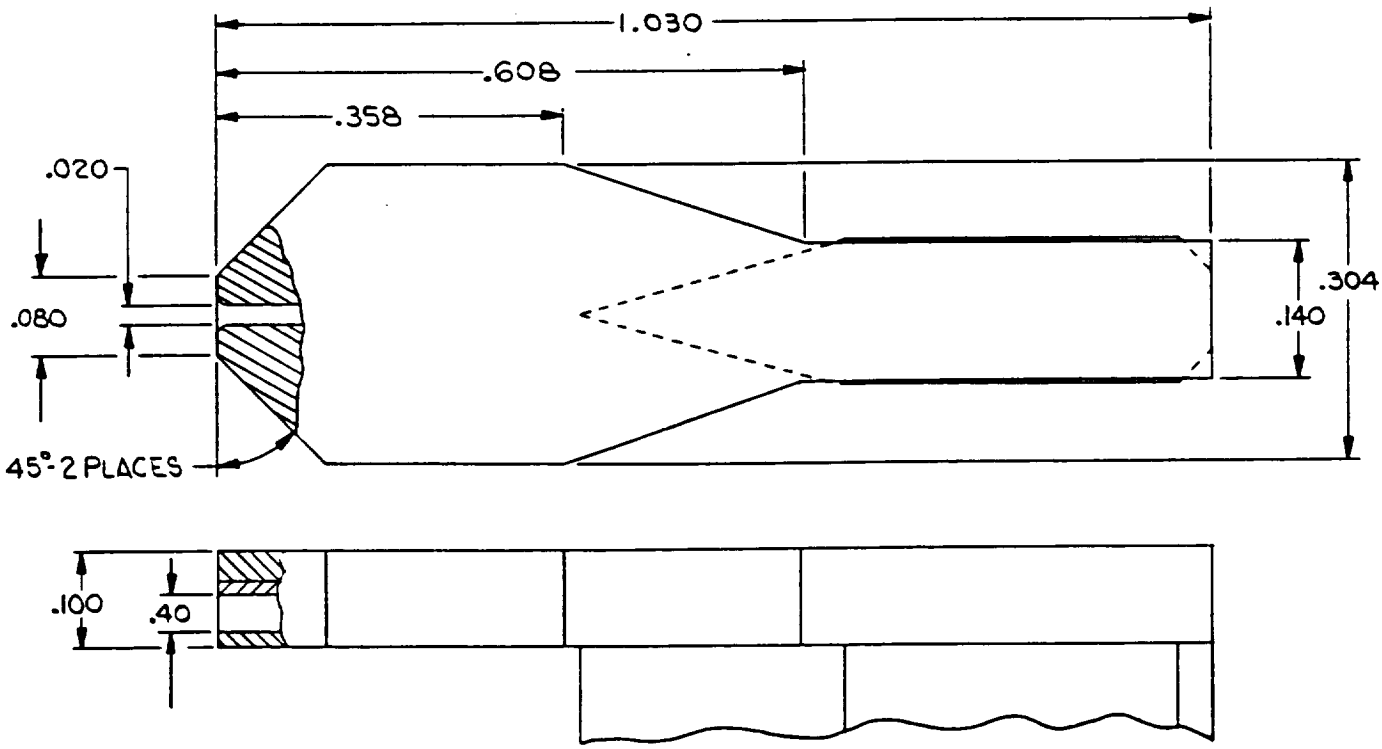

High Temperature Probe Dimensions
Figure A-5

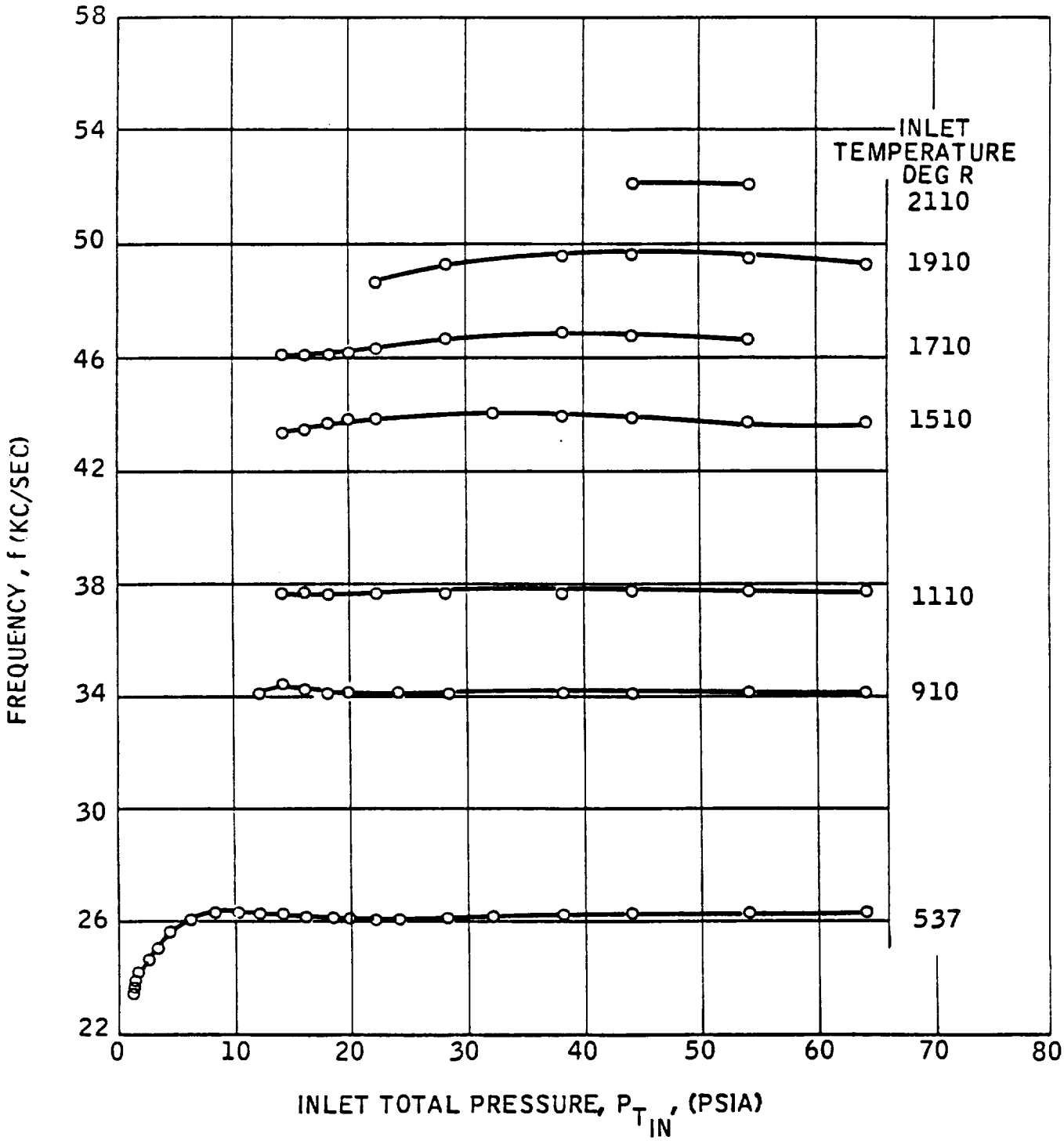

Characteristic Plot, Probe B: Frequency vs Inlet Total Pressure
Figure A-6

Material and Fabrication Considerations

While the fundamental consideration in choosing a material for the temperature oscillators was the temperature environment, the means of fabrication also played into the material choice. Considerable effort was expended in an attempt to weld the sensor components into a monolithic assembly. Thus, weldability and a tendency to distort under thermally induced welding stresses were initially a major factor in material selection. Despite a great deal of effort in this area, diffusion bonding ultimately proved to be the only practical means of assembly and capability for diffusion bonding was an important material selection criterion.

The low temperature and high temperature sensors were built from different materials. The low temperature (up to 2300 deg.R) sensors were designed for long term (100 hours) service. The high temperature probes (to 4500 deg.R) were designed to function for only ten minutes.

Low Temperature Probes

The following materials were given close scrutiny for use in the low temperature application:

* Stainless steels of various compositions
* Thoria Dispersed Nichrome
* Inconel X
* Inconel 702
* Nickel
* Multimet
* Chrome 30
* Hasteloy X

Samples of appropriate shape were tested in flames produced by either a Linde jet piercing torch, fueled with oxygen and kerosene, or an oxyacetylene torch. Of the materials tested, only TD Nichrome and Chrome 30 showed adequate stability for long term servce. However, at the time, the TD Nichrome was in early development and not available in sufficient quantities. The delivery schedule for the low temperature probes prevented selection of the Chrome 30 because its machining characteristics and diffusion bonding capability had not been sufficiently explored.

Inconel 702 was chosen for the low temperature probes although the rate of oxidation curves from the torch testing showed the approach of adverse changes at the 100 hour point. Inconel 702 was readily machinable, weldable and diffusion bonding development with the material proved successful.

High Temperature Probes

The high temperature probes were intended for use in blow-down wind tunnels which brought the aspect of thermal shock into the material selection process. Blunted wedges, the shape of

concern in the temperature oscillator, were exposed to the torch testing under cyclic conditions; 10 second exposure for 60+ cycles. The cyclic testing along with 10 minute exposure at 3500 deg.R was used to determine suitable materials.

These tests isolated Chrome 30 as the only material suitable for the high temperature probes. While Chrome 30 would not survive operation at 4500 deg.R, laboratory testing showed it to be satisfactory at 3500 deg.R. Fabrication was difficult... Chrome 30 is brittle and extreme care was required in handling the small parts through the many grinding and surfacing operations required for successful diffusion bonding of the tiny parts. Five separate diffusion bonding operations were required for the complete assembly.

Performance

The various limitations of the testing process in the laboratory lead to a series of compromises in the calibration process. The curves of frequency vs inlet total temperature as shown in figure A-6 for Probe B were fitted with an empirical equation resulting in a straight line plot of nominal values as shown in figure A-7. These lines were then regarded as "nominal values" and the accuracy of a given probe was treated as the percentage difference between calculated temperature for the probe. The results are shown in Table A-1

Percent Errors Between Nominal And Calculated Temperatures For Probe B Inlet Pressure range 7.5 To 80 psia

Temperature Degrees R	Error Percent	Temperature Degrees R	Error Percent
535	0	1710	1.58
910	0.77	1910	0.58
1110	0.13	2110	0.14
1510	1.00		

A similar log log plot of the high temperature probe characteristic is shown in figure A-8, valid for inlet total pressures between 0.5 and 2.0 atmospheres. Performance for two different high temperature probes is shown in figure A-9. These data were measured in the NASA Ames 3.5 foot hypersonic wind tunnel.The plot compares data from the fluid temperature probes with data from a triple shielded, Rosemount Engineering Corporation platinum/platinum-rhodium thermocouple. The fluctuations in temperature values measured by the fluid probe are attributed to the more rapid response of the fluid probe as compared to the more damped thermocouple response.

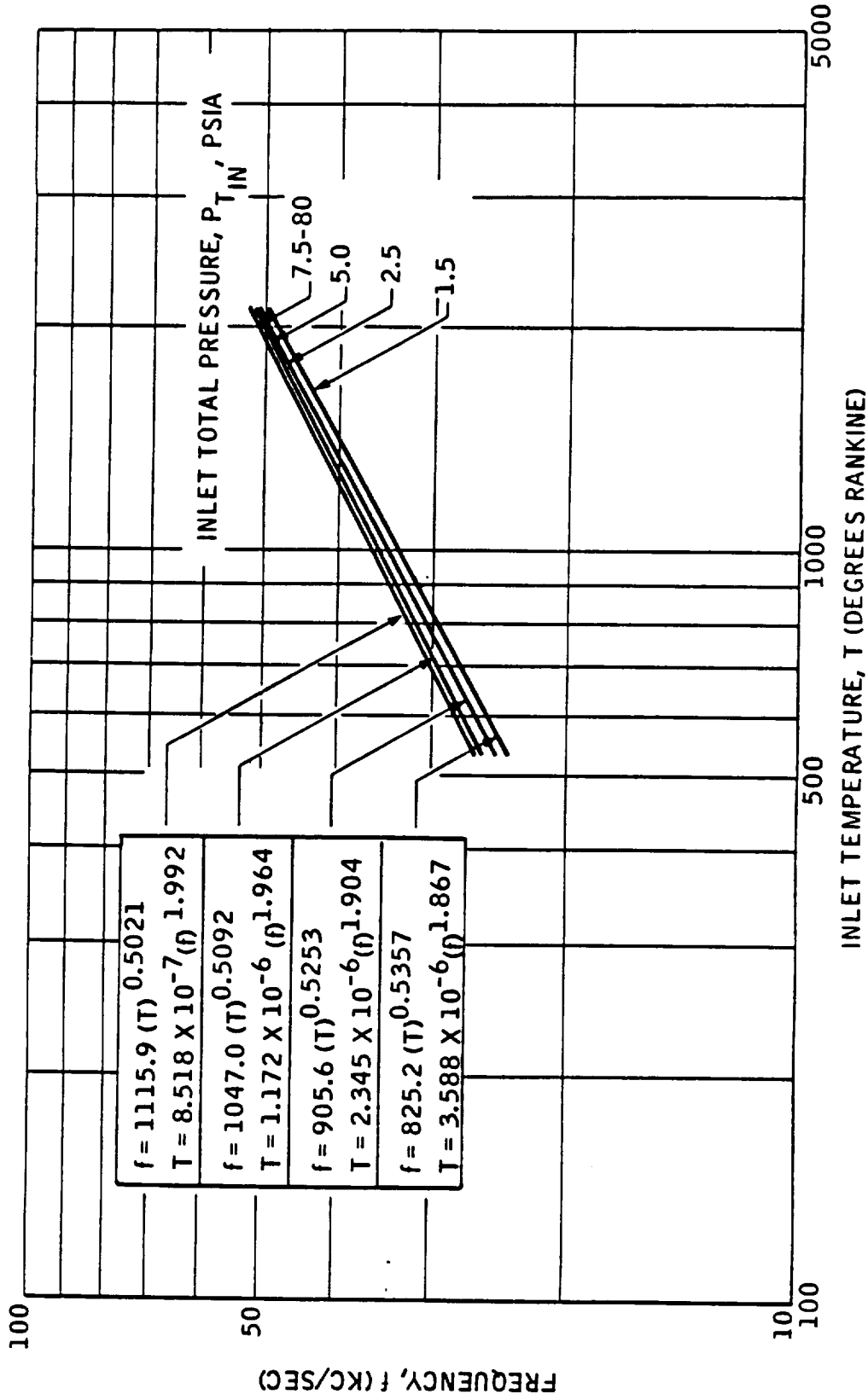

Frequency vs Inlet Temperature, Probe B
Figure A-7

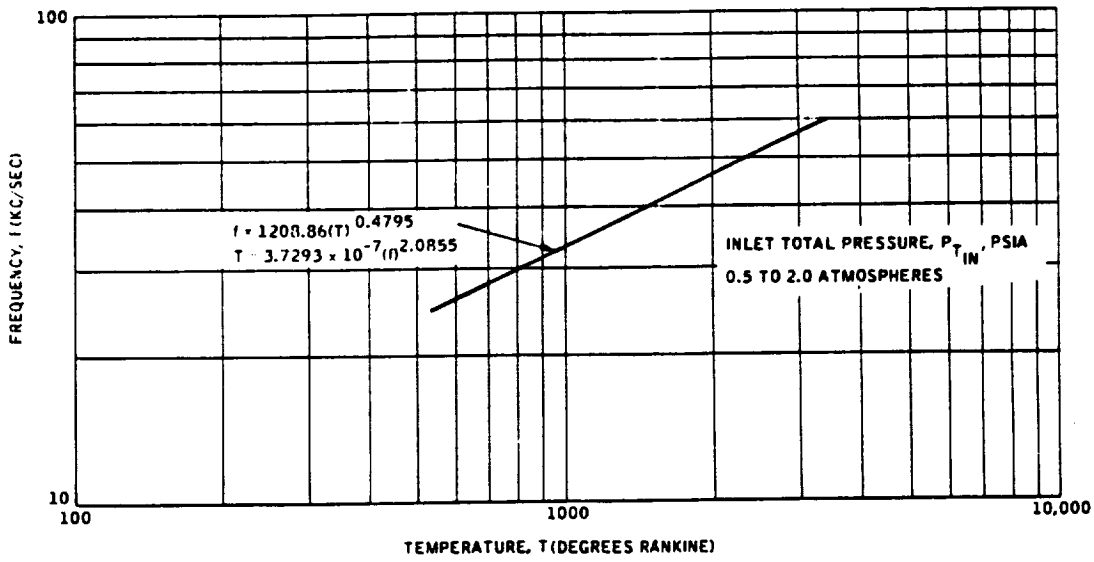

Frequency vs Inlet Temperature, Probe C
Figure A-8

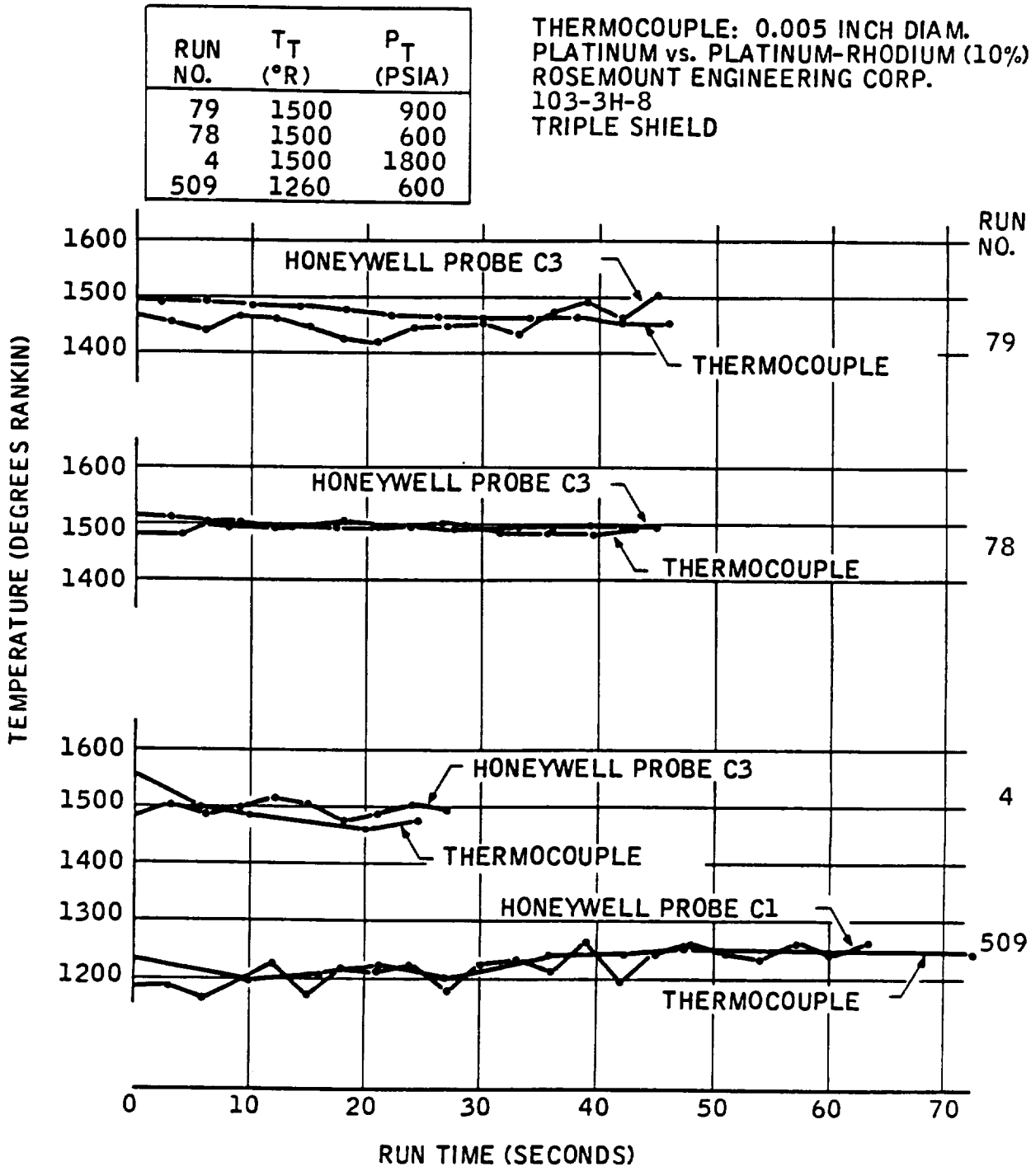

Temperature vs Run Time, Probes C1 and C3 At Mach 7.4 In Ames Hypersonic Tunnel
Figure A-9

X-15 TEMPERATURE PROBE

The operating conditions of X-15 aircraft dictated an entirely different design philosophy for the fluid temperature probe to be used in flight operations. The flight environment allowed a flow-through design while maintaining a choked flow downstream of the sensor cavity. Air whose temperature is to be measured enters the sensor through a small orifice in the forward stagnation region and exits into the base region, figures A-10 and A-11.

In flight, heat is transferred from the hot air to the sensor body and, as a result, the sensor must be cooled to maintain its integrity. Nitrogen gas is passed through the sensor body, entering through the mounting pylon and dumped overboard in a low pressure region around the sensor. The nitrogen is not permitted to mix with the incoming flow.

The cooled sensor body also cools the flow whose temperature is to be measured. This requires that a correction factor to be applied to the basic frequency measurement. The correction factor is a function of the body temperature which was measured with a chromel-alumel thermocouple located at the rear of the body cavity as shown in figure A-10.

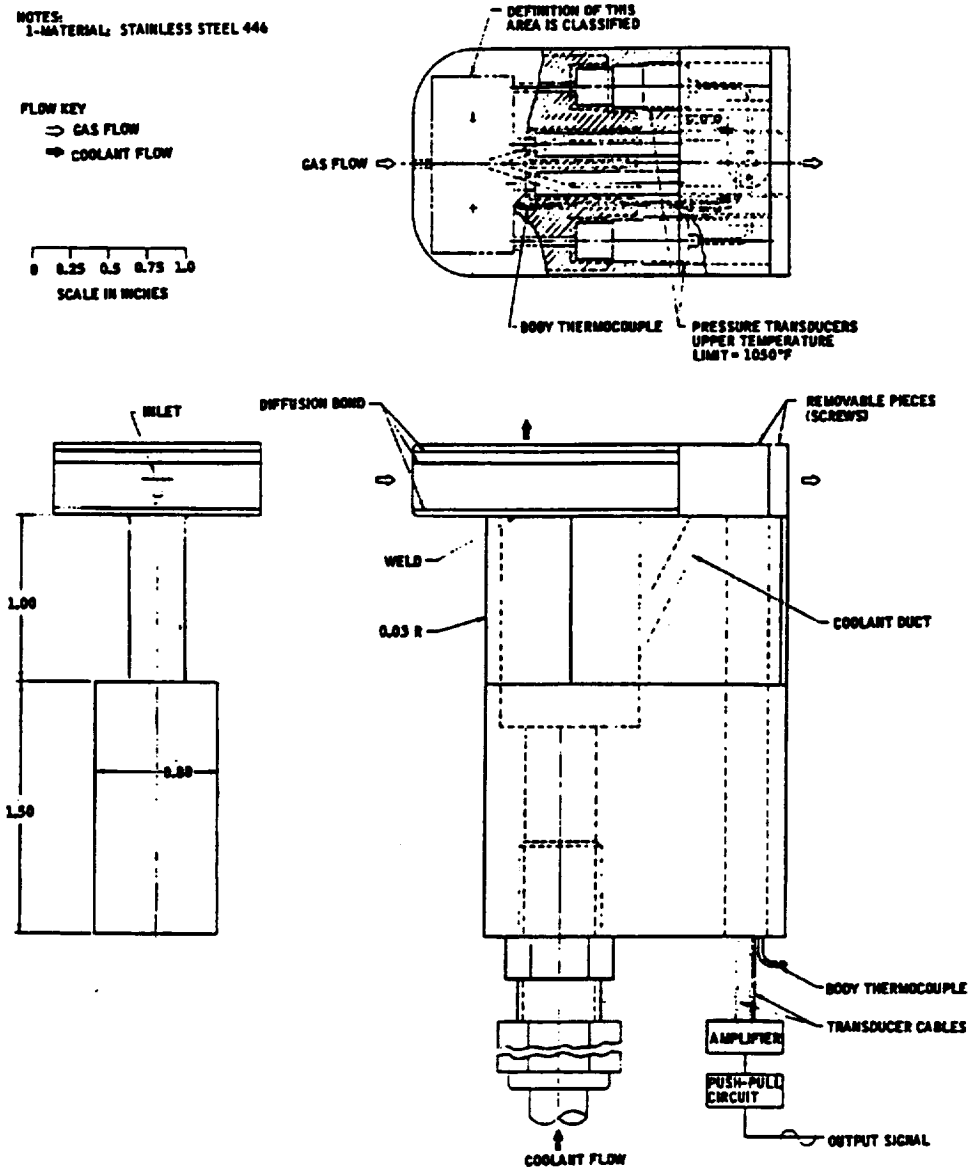

X-15 High Temperature Probe
Figure A-10

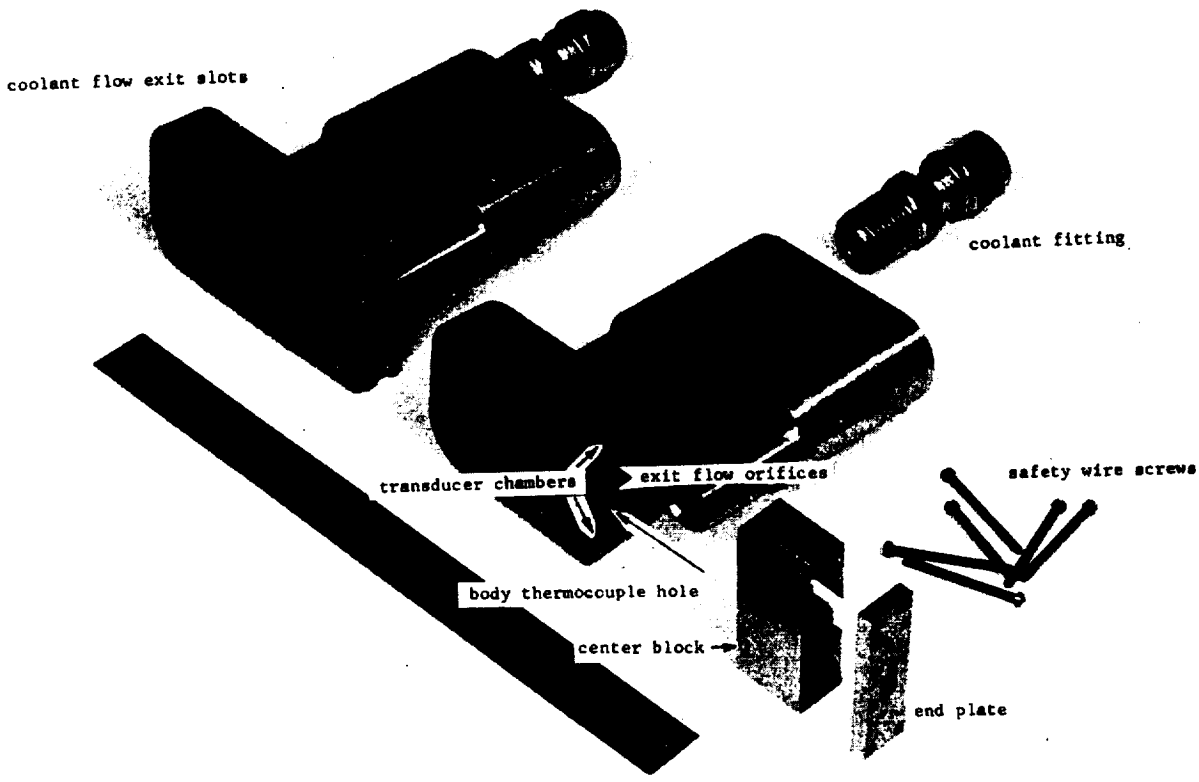

X-15 Probe, Assembled and Disassembled

Figure A-11

APPENDIX B

REFERENCES

1. Keenan, Joseph H., and Kaye, Joseph: *Thermodynamic Properties of Air, Products of Combustion and Component Gases*. John Wiley & Sons, Inc. New York, 1949.

2. Staff of Applied Physics Laboratory; Handbook of Supersonic Aerodynamics, Volume 5; Mechanics of Rarefied Gases. Bureau of Naval Ordnance Report 1488 (Vol. 5), 1950

3. Herrington, Russel M., et al.: Flight Test Engineering Handbook. U.S. Air Force Flight Test Center, Edwards, CA, 1980

4. Courtright, E.L. et al.: Ultrahigh Temperature Assessment Study - Ceramic Matrix Composites, WL-TR-91 Materials Directorate, Wright Laboratories, Wright-Paterson Air Force Base, Ohio, March, 1991.

5. Sheehan, James E., High-Temperature Coatings on Carbon Fibers and Carbon-Carbon Composites. Chapter 8, Carbon-Carbon Materials and Composites, NASA Reference Publication, February, 1992.

6. Ewart, L. and Suresh, S.; Crack Propagation in Ceramics Under Cyclic Load. *Journal of Material Science*, Volume 22, 1987.

7. Personal Communication; Mark Dowell. Union Carbide Company, Advanced Ceramics Division, Cleveland, OH, October, 1992.

8. Technical Information Bulletin. Union Carbide Company, Advanced Ceramics Division, Cleveland, OH, undated.

9. Personal Communication; Dr. Jerry Wittenauer. Lockheed Missiles and Space Co. Sunnyvale, CA, November, 1992.

10. Packer, C.M.; Overview of Silicide Coatings for Refractory Metals. In *Oxidation of High-Temperature Intermetallics*, The Minerals, Metals and Materials Society, 1989, p. 235–244.

11. Bailey, R. G., et al: A Study of All-Fluid Temperature Sensing Probes. Honeywell Inc., Minneapolis, Minn., 1967. Also available as NASA CR-90092.

APPENDIX C

SOURCES OF CARBON/CARBON MATERIALS

The following is a list of suppliers/fabricators of carbon/carbon composite materials.

B.P. Chemical Garden Grove, CA Norbert Meyer	213 516 5770
Fiber Materials Inc. Biddeford, ME Jack Smith	207 282 5911
B.F. Goodrich Santa Fe Springs, CA William Pfeifer	213 944 6244
Kaiser Aerotech San Leandro, CA H.O. Davis	415 562 2456
Rohr Corporation San Diego, CA Thomas Spamer	619 691 3193
RTAC Magna, UT Perry Bruno	801 251 1390
Science Applications International Santa Ana, CA No contact	714 542 9411
Textron Specialty Materials Lowell, MA Arthur Taverna	508 567 2438

APPENDIX D

PRESSURE TRANSDUCER MANUFACTURERS

The following is a list of pressure sensor manufacturers contacted with regard to high temperature, high frequency response transducers with maximum sensitivity.

A.L. Design
1411 Military Road
Buffalo, NY 14217-1305

Barksdale Controls Division
IMO Industries, Inc.
3211 Fruitland Avenue
Los Angeles, CA 90058

Channel Industries
839-T Ward Drive
Santa Barbara, CA 93102

Daytran Instruments, Inc.
21592 Marilla St.
Chatsworth, CA 91311

Entran Sensors & Electronics
10Washignton Avenue
Fairfield, NJ 07004

Etalon Inc.
104 N. Church Street
Box 40
Lizton, IN 46149

IMO Industries Inc.
CEC Instruments Division
955 Overland Court
P.O. Box 901
San Dimas, CA 91773

ICSensors
1701 McCarthy Boulevard
Milpitas, CA 95035-7416

Kavilco Corporation
14501 Los Angeles Avenue
Moorpark, CA 93021

Keramos Inc.
5460 West 84th Street
Indianapolis, IN 46268

Kistler Instrument Corp.
75 John Glenn Drive
Amherst, NY 14228-2171

PCB Piezotronics, Inc.
3425 Walden Avenue
Depew, NY 14043-2495

Sensotron
5881 Engineer Drive
Huntington Beach, CA 92649

Sensym Inc.
1244-T Reamwood Avenue
Sunnyvale, CA 94089

APPENDIX E

BIBLIOGRAPHY

McAdams, William H.: *Heat Transmission*. McGraw-Hill Book Company, Inc., New York, 1942.

Gibbs, Charles W.: Compressed Air and Gas Data. Ingersoll-Rand Company, Woodcliff Lake, NJ, 1971.

Staff of Applied Physics Laboratory: Handbook of Supersonic Aerodynamics, Volume 2; Compressible Flow Tables and Graphs. Bureau of Naval Ordnance Report 1488 (Vol. 2), 1950

Schapiro, Ascher H.: *The Dynamics and Thermodynamics of Compressible Fluid Flow.* The Ronald Press Company, New York, NY, 1953.

Blakslee, O.L., Proctor, D.G., Seldin, E.J., Spence, G.B., and Weng, T.: Elastic Constants of Compression Annealed Pyrolytic Graphite. *Journal of Applied Physics*, vol. 41, no. 8, July 1970.

Kibler, John J.: Mechanics of Multidirectional Carbon-Carbon Composite Materials. Chapter 6, Carbon-Carbon Materials and Composites, NASA Reference Publication, February, 1992.

Marshall, D.B. and Evans, A.G.; Failure Mechanisms in Ceramic-Fiber/Ceramic-Matrix Composites. *Journal American Ceramic Society* 68(5), 1985.

Gets, Michael W. and Angus, John C.: Diamond Film Semiconductors. *Scientific American*, October, 1992.

Wittenauer, J.P., Nieh, T.G. and Wadsworth, Jeffrey: Tungsten and Its Alloys. *Advanced Materials and Processes*, September, 1992.

REPORT DOCUMENTATION PAGE

Form Approved
OMB No. 0704-0188

1. AGENCY USE ONLY *(Leave blank)*	2. REPORT DATE	3. REPORT TYPE AND DATES COVERED
	June 1993	Contractor Report

4. TITLE AND SUBTITLE

Program for an Improved Hypersonic Temperature-Sensing Probe

5. FUNDING NUMBERS

WU 505-68-50
NAS2-13457

6. AUTHOR(S)

Richard J. Reilly

7. PERFORMING ORGANIZATION NAME(S) AND ADDRESS(ES)

Cuyuna Corporation
3909 Peak Lookout Drive
Austin, Texas 78738

8. PERFORMING ORGANIZATION REPORT NUMBER

H-1893

9. SPONSORING/MONITORING AGENCY NAME(S) AND ADDRESS(ES)

National Aeronautics and Space Administration
Washington, DC 20546-0001

10. SPONSORING/MONITORING AGENCY REPORT NUMBER

NASA CR-186025

11. SUPPLEMENTARY NOTES

NASA Technical Monitor: Rod Bogue, Dryden Flight Research Facility, Edwards, California

12a. DISTRIBUTION/AVAILABILITY STATEMENT

Unclassified — Unlimited
Subject Category 35

12b. DISTRIBUTION CODE

13. ABSTRACT ***(Maximum 200 words)***

Under a NASA Dryden-sponsored contract in the mid 1960s, temperatures of up to 2200 °C (4000 °F) were successfully measured using a fluid oscillator. The current program, although limited in scope, explores the problem areas which must be solved if this technique is to be extended to 10,000 °R. The potential for measuring extremely high temperatures, using fluid oscillator techniques, stems from the fact that the measuring element is the fluid itself. The containing structure of the oscillator need not be brought to equilibrium temperature with the fluid for temperature measurement, provided that a suitable calibration can be arranged. This program concentrated on review of high-temperature material developments since the original program was completed. Other areas of limited study included related pressure instrumentation requirements, dissociation, rarefied gas effects, and analysis of sensor time response.

14. SUBJECT TERMS

Temperature sensors, High temperature, Fluid oscillator

15. NUMBER OF PAGES
60

16. PRICE CODE
A04

17. SECURITY CLASSIFICATION OF REPORT	18. SECURITY CLASSIFICATION OF THIS PAGE	19. SECURITY CLASSIFICATION OF ABSTRACT	20. LIMITATION OF ABSTRACT
Unclassified	Unclassified	Unclassified	Unlimited